

Article

Validation of Two Theoretically Derived Equations for Predicting pH in CO₂ Biomethanisation

Yue Zhang , Sonia Heaven  and Charles J. Banks 

Water and Environmental Engineering Group, Faculty of Engineering and Physical Sciences,
University of Southampton, Southampton SO16 7QF, UK

* Correspondence: Y.Zhang@soton.ac.uk (Y.Z.); S.Heaven@soton.ac.uk (S.H.)

Abstract: CO₂ biomethanisation is a rapidly emerging technology which can contribute to reducing greenhouse gas emissions through the more sustainable use of organic feedstocks. The major technical limitation for in situ systems is that the reaction causes CO₂ depletion which drives up pH, potentially leading to instability and even digestion failure. The study aimed to test fundamentally derived predictive equations as tools to manage H₂ addition to anaerobic digesters. The methodology used data from the literature and from experimental digesters operated with excess H₂ to a point of failure and subsequent recovery. Two equations were tested: the first relating pH to CO₂ partial pressure (pCO₂), and the second extending this to include the influence of volatile fatty acids and ammonia. The first equation gave good agreement for data from studies covering a wide range of operating conditions and digester types. Where agreement was not good, this could usually be explained, and in some cases improved, using the second equation, which also showed excellent predictive performance in the experimental study. The results validated the derived equations and identified typical coefficient values for some organic feedstocks. Both equations could provide a basis for process control of CO₂ biomethanisation using routine monitoring of pH or pCO₂ with additional analysis for volatile fatty acids and total ammonia nitrogen when required.

Keywords: CO₂ biomethanisation; pH change; CO₂ partial pressure; volatile fatty acids; ammonia



Citation: Zhang, Y.; Heaven, S.; Banks, C.J. Validation of Two Theoretically Derived Equations for Predicting pH in CO₂ Biomethanisation. *Processes* **2023**, *11*, 113. <https://doi.org/10.3390/pr11010113>

Academic Editor: Blaž Likozar

Received: 4 December 2022

Revised: 22 December 2022

Accepted: 24 December 2022

Published: 31 December 2022



Copyright: © 2022 by the authors. Licensee MDPI, Basel, Switzerland. This article is an open access article distributed under the terms and conditions of the Creative Commons Attribution (CC BY) license (<https://creativecommons.org/licenses/by/4.0/>).

1. Introduction

The ability of certain methanogens to use hydrogen (H₂) as a reducing agent for the conversion of carbon dioxide (CO₂) into methane (CH₄) has been known to science for decades [1]. More recently, the growing realisation of the potential engineering applications has helped to move this process rapidly up through technology readiness levels from the initial laboratory research [2] to larger-scale implementation [3,4]. CO₂ biomethanisation can be carried out in various configurations. Ex situ processes are usually defined as operating on gaseous H₂ and CO₂ in dedicated reactors, with or without defined inocula, and can offer the advantages of high gas transfer rates and volumetric throughput: the main commercial systems currently in use are of this type [3–5]. In situ systems use CO₂ produced during the anaerobic digestion of organic substrates, with the addition of H₂ stimulating parts of the mixed microbial community to carry out the CO₂ biomethanisation process. Various hybrids of these two basic concepts are also possible, e.g., where additional exogenous CO₂ is provided for conversion within an in situ system [6], or where high-rate reactors are fed with organic substrates for nutrient supply and/or replenishment of the microbial population, rather than as the main source of CO₂ [7,8]. Other variants under development include those using syngas [9], zero-valent iron [10], and bioelectrochemical systems [11].

While ex situ systems are furthest along the pathway to full-scale application, all these approaches have specific advantages and features that make them suited to different applications. The urgent need for renewable hydrocarbons and for more sustainable utilisation of organic carbon has recently led to increasing interest in biomethanisation of CO₂ from waste

feedstocks, as evidenced by a growing number of papers on this topic [12]. The attractions of this approach are firstly that it can enhance CH₄ yields from existing AD infrastructure, with potentially low retrofitting costs [13]. Secondly, it increases the scope for the integration of anaerobic digestion with local or grid-based renewables and other on-site technologies [14,15]. Thirdly, it can provide biogas with a high methane content, in some cases equal to that reported for single-pass ex situ reactors [12], from organic carbon inputs.

The main perceived drawback of the in situ approach is that reduction in the headspace CO₂ content induces a rise in pH [16], which if uncontrolled can lead to process instability or even digestion failure [17,18]. In full-scale digesters this is expensive and time-consuming to rectify: in the worst case, digester contents may have to be replaced with fresh inoculum, leading to extended downtime, and a digestate disposal problem [19]. As with other process innovations, widespread adoption of CO₂ biomethanisation will require companies to have confidence in their ability to control the process and to avoid any risk of instability, or to identify and deal with it for some reason it does occur. This security can be delivered by the development of effective process control tools [20,21], which ideally should be based on experimentally validated relationships that are underpinned by sound science and an in-depth understanding of the factors involved [22]. To be accepted, such relationships must also be demonstrated as robust over a wide range of conditions, including periods of dynamic change and when operations become unstable, e.g., with accumulation of volatile fatty acids (VFA) [20,22].

As a step towards this, Tao et al. [6] suggested a relationship between digester pH and partial pressure of CO₂ (pCO₂) in the headspace that would allow estimation of the minimum pCO₂ for stable operation, and thus by extension, the maximum achievable CH₄ content. The strength of this lies in the fact that it is derived from fundamental principles and requires only minimal information (digester operating temperature and a baseline value for pH and pCO₂) for calibration and use. It was developed for systems where ammonium-bicarbonate buffering is dominant, as is the case for most real-world organic feedstocks. Although, extension to phosphate, which is usually present when basal media are used, was also demonstrated [6]. However, it did not include consideration of VFA which may accumulate during CO₂ biomethanisation for various reasons, e.g., too high a H₂ partial pressure and/or too high pH without appropriate acclimatisation. The authors were also unable to explain why the maximum acceptable pH seemed to vary with different substrates, and more work is needed to clarify this.

In the current work, data gathered from an extensive review of published literature was used to investigate how well the original equation derived by Tao et al. [6] was able to predict operating pH from pCO₂, and where the fit was poor, to see whether it was possible to understand why. The original equation was modified to include consideration of the effects of total ammonia nitrogen (TAN) and VFA, and where suitable literature data were available these were used to test and compare the performance of the two equations. As the number of studies with suitable data was limited, both equations were also applied to data from a laboratory-scale CO₂ biomethanisation trial which was deliberately designed to show VFA accumulation and the onset of process instability.

The results from all parts of this work clearly demonstrated the robustness of the derived equations, and thus their potential suitability for use in process control systems based on pCO₂ and/or pH measurements, with additional monitoring of TAN and VFA when required.

2. Materials and Methods

2.1. Equations Relating pH and pCO₂

The equation derived by Tao et al. [6] relates pH to the partial pressure of CO₂ in the digester headspace

$$pH = -\log_{10} \left(\frac{a \cdot p_{CO_2} + \sqrt{a^2 \cdot p_{CO_2}^2 + 4 \cdot 10^{-t} \cdot a \cdot p_{CO_2}}}{2} \right) \quad (1)$$

where:

$$a = \frac{(10^{-pH^0})^2}{10^{-t} + 10^{-pH^0}} \cdot \frac{1}{p_{CO_2}^0} \quad (1a)$$

$$t = 0.90018 + \frac{2729.29}{T} \quad (1b)$$

and T is the digester operating temperature digester in degrees K.

The superscript 0 in Equation (1a) represents chosen baseline values. Symbols with this superscript are therefore constants obtained from a control digester or operating period, e.g., from conventional anaerobic digestion without CO_2 biomethanisation.

The above relationship can be taken further by considering the effect of VFA. As weak acids, these metabolic products are also capable of donating protons to NH_3 in an AD environment. A modified version of Equation A can therefore be obtained, which applies to both baseline conditions and in CO_2 biomethanisation.

At equilibrium:

$$[HCO_3^-] + [VFA^-] = [NH_4^+] \quad (2a)$$

where [] represents molar concentration.

Among the terms in Equation (2a)

$$[HCO_3^-] = \frac{K_{a1}K_H p_{CO_2}}{10^{-pH}} \quad (2b)$$

(as in Equation (4) in Tao et al. [6]), and

$$[NH_4^+] = \frac{10^{-pH}}{10^{-t} + 10^{-pH}} [TAN] \quad (2c)$$

(as in Equation (7) in Tao et al. [6], but with t left as a variable rather than expressed as the constant for operation at 37 °C).

Considering that the pH of anaerobic digestion processes is commonly neutral or slightly in the alkaline range, especially under CO_2 biomethanisation:

$$[VFA^-] = [VFA] \quad (2d)$$

where [VFA] represents total VFA concentration, including both protonated and deprotonated forms.

Equation (2a) can then be converted to:

$$\frac{K_{a1}K_H p_{CO_2}}{10^{-pH}} + [VFA] = \frac{10^{-pH}}{10^{-t} + 10^{-pH}} [TAN] \quad (2e)$$

Therefore:

$$\left(10^{-pH}\right)^2 - \frac{K_{a1}K_H p_{CO_2} + [VFA] \cdot 10^{-t}}{[TAN] - [VFA]} \cdot 10^{-pH} - \frac{K_{a1}K_H p_{CO_2} \cdot 10^{-t}}{[TAN] - [VFA]} = 0 \quad (2f)$$

Solving Equation (2f) gives:

$$10^{-pH} = \frac{(b \cdot p_{CO_2} + [VFA] \cdot 10^{-t}) + \sqrt{(b \cdot p_{CO_2} + [VFA] \cdot 10^{-t})^2 - 4 \cdot ([TAN] - [VFA]) \cdot (-b \cdot p_{CO_2} \cdot 10^{-t})}}{2 \cdot ([TAN] - [VFA])} \quad (2g)$$

where:

$$b = K_{a1}K_H = \left(\frac{10^{-pH^0}}{10^{-t} + 10^{-pH^0}} [TAN]^0 - [VFA]^0 \right) \cdot \frac{10^{-pH^0}}{p_{CO_2}^0} \quad (2h)$$

Therefore, the relationship between pH and p_{CO_2} can be expressed as in Equation B:

$$pH = -\log_{10} \frac{(b \cdot p_{CO_2} + [VFA] \cdot 10^{-t}) + \sqrt{(b \cdot p_{CO_2} + [VFA] \cdot 10^{-t})^2 - 4 \cdot ([TAN] - [VFA]) \cdot (-b \cdot p_{CO_2} \cdot 10^{-t})}}{2 \cdot ([TAN] - [VFA])} \quad (2)$$

For the remainder of this paper the expressions shown in Equations (1) and (2) are referred to as Equation A and Equation B, respectively. When the VFA concentration is zero, Equation B is identical to Equation A. It should be noted that Equation B does not apply when the molar concentration of VFA is close to or greater than that of TAN as, in this case, the ammonia produced is not sufficient to neutralise both fatty acids and carbonic acid.

2.2. Literature Data

Search terms including ‘CO₂ biomethanisation’ or ‘CO₂ biomethanation’, ‘in situ biogas upgrading’, and ‘anaerobic digestion’ in conjunction with ‘H₂ addition’ were used to identify papers of possible interest. This produced several thousand publications, the majority of which after a brief inspection of the title or abstract were found not to be relevant to the current study. A total of 73 papers, identified either directly in this way or from the reference lists of the selected papers, were examined in more detail. In total, 37 of these were eliminated as they did not directly address in situ conversion of CO₂ from organic feedstocks, did not include the required data on pH and pCO₂, or for other methodological reasons. Data were then extracted from the remaining 36 peer-reviewed papers and their supporting materials, with additional information obtained from the authors where possible.

The resulting data were in the form of sets of average values from different experimental periods in a study, or individual points from experimental data series. For each study or dataset considered, average values for pH, pCO₂, and where available VFA and TAN concentrations from control reactors or baseline periods were used to derive coefficients *a* or *b* for Equations A or B. Measured CO₂ concentrations were then used to predict pH for each data point, excluding the selected control or baseline period, for comparison with experimental pH values.

2.3. Digester Set-Up and Operation

Experimental work was carried out in eight 1-L digesters (designated D1-8) maintained at 37 °C in a water bath, as described in Tao et al. [23]. The digesters were mixed by 40 mm diameter 3-blade impellers driven at 200 rpm. Each digester initially received 500 mL of inoculum from a mesophilic anaerobic digester at Millbrook Wastewater Treatment Works (WWTW), Southampton, UK. The feed was co-settled primary and secondary sewage sludge collected from Budds Farm WWTW, Portsmouth, UK, in a single batch and frozen in aliquots until required, then stored under refrigeration until use. The average total solids (TS) content of the feed was 6.91% wet weight (WW) with average volatile solids (VS) of 5.69%WW. Feeding and digestate removal were carried out manually once per day to give a Hydraulic Retention Time (HRT) of 14.6 days and an organic loading rate (OLR) of 3.87 g VS L⁻¹ day⁻¹ unless noted. All digesters had been run under these conditions for 70 days before the start of the current trial to ensure stable and replicable operation. From day 0–54, operation of all digesters continued under the same conditions to allow the establishment of robust baseline values.

H₂ addition was achieved by dispensing the required volume into a foil-lined gas-impermeable bag using an EL-Flow Prestige mass flow controller (Bronkhorst, UK). The filled gas bag was attached to the digester immediately after the daily addition of organic feed, and the gas was bubbled up through the digestate and recirculated from the headspace at a flow rate of 8 mL min⁻¹. At the end of the daily cycle, the full gas bag was removed for measurement of gas volume and composition.

In general, gas production and composition were measured daily throughout the experiment. From day 0–54 pH and VFA concentrations were measured twice a week, with

TAN, alkalinity, and solids content measured weekly. pH and VFA were measured daily between days 55–100, covering the period of H₂ addition and subsequent stabilisation, while other parameters were measured intermittently. More frequent monitoring was resumed at the end of the experimental period from day 110–125.

2.4. Analytical Methods

TS and VS were determined by Standard Method 2540 G [24]. TAN was measured using a BÜCHI K-350 Distillation Unit, with NaOH addition followed by titration of the distillate in a boric acid indicator with 0.25 N H₂SO₄. Alkalinity was measured using a SCHOTT titroline system with titration by 0.25 N H₂SO₄ to endpoints of pH 5.75 and 4.3, to allow calculation of total (TA), partial (PA), and intermediate alkalinity (IA) [25]. VFA concentrations were determined by gas chromatography (Shimadzu GC-2010) using a flame ionisation detector and a capillary column (SGE BP-21) with nitrogen as the carrier gas. Samples were acidified to 10% with formic acid and quantified against mixed standards of 50, 250, and 500 mg L⁻¹ of acetic, propionic, iso-butyric, n-butyric, iso-valeric, valeric, hexanoic, and heptanoic acids. Biogas composition was determined using a MG#5 Gas Chromatograph (SRI Instruments, Torrance, CA, USA) with a thermal conductivity detector (TCD). The instrument had two linked analytical lines with CH₄ and CO₂ separated by a Porapak Q column (80/100 mesh, 6ft), and H₂ by a molecular sieve 5A column (6ft). GC calibration was conducted using standard gases supplied by BOC, UK. Gas volumes were determined in a weight-based water displacement system [26] and are reported as dry gas at a standard temperature and pressure (STP) of 0 °C and 101.325 kPa.

2.5. Performance Assessment and Statistical Analyses

Performance of Equations A and B was assessed by several measures. Heat maps were used to show the absolute value of the difference between experimental and predicted pH for single data points or for average values for an experimental period. For multiple values, in the first instance the Root Mean Square Deviation was calculated, with deviation defined here as the difference between experimental pH and predicted pH value for each point.

Where data points might be expected to show some relationship, e.g., between average values for different sets of conditions within an experiment or between individual points in a data series, regression analysis was carried out. For this purpose, the coefficient of determination (R²) and the Root Mean Square Error (RMSE) were calculated, with error defined as the difference between the predicted pH and the line of best fit for experimental and predicted values, to take account of variation in experimental values. The slope and intercept of regression equations were also considered. T-tests were used to determine the significance of regression statistics and of differences between slopes, with values taken as significant at the 5% level.

For the purposes of assessment, the level of agreement between experimental and predicted pH was defined as good if the difference was <0.1, reasonable between 0.1–0.2, and poor if >0.2 for single data points, or for the RMSD or RMSE of multiple values. Correlation between predicted and experimental pH was defined as poor for R² < 0.8, reasonable for R² between 0.8–0.9, and good for R² > 0.9. These definitions were based on examination of the data and consideration of likely measurement accuracy [24,27]. The studies considered were not specifically designed for the evaluation of the relationship between pH and pCO₂ and would therefore not have taken any special steps to ensure accuracy. pH values are affected by temperature and dissolved CO₂ content, which may change after removal of the sample from the digester [19], while online in-situ measurement requires frequent calibration for accuracy [19]. As a non-combustible gas, it is also challenging to measure CO₂ accurately over the wide range of partial pressures found in CO₂ biomethanisation experiments, whether by gas chromatography (GC) or sensor [27]. The precision of the available data was also taken into account, with, e.g., pH values often only reported to 0.1 unit in AD and CO₂ biomethanisation studies.

3. Results

3.1. Application of Equation A to the Literature Data

In total, 36 studies were found with suitable data on pH and $p\text{CO}_2$. Most of these reported average values for monitoring parameters from periods of operation under specified conditions, often supported by graphical data. Some also provided numerical data in Supplementary Materials or on request.

The studies covered a wide range of experimental conditions and operating configurations, including different digester types (continuous stirred tank reactors (CSTR) [6,17,18,23,28–52], upflow anaerobic sludge blanket (UASB) reactors [53,54], anaerobic membrane bioreactors (An-MBR) [55,56], and anaerobic filters (AF) or trickle beds [57,58]. These were arranged in single and 2-stage systems with H_2 injection in the first [59] or second [32,36,42,43,45–47,60] stage, and with [59] or without [32,42] gas recirculation between the stages). Rates of mixing, gas addition, and recirculation were also varied both within and between studies. Some studies were carried out in pressurised systems [35,37], with gases other than H_2 (e.g., carbon monoxide [41,54] or syngas [48,49]). Different gas supply systems were used, including headspace injection [28,29,47,58], various types of bubble tube [6,23,34] or diffuser [2,32,37,42,44,46,49,50,54], venturi outlets [57], and membrane systems [30,40,48]. Trials were conducted in mesophilic [28–30,33–38,44,48,52,54–56,58] and thermophilic [17,18,31,39–47,50,53,59,60] conditions, in some cases specifically to compare these [32,49,51]. They were also performed with a variety of feedstocks including livestock manures and slurries, crop and agro-wastes, industrial and post-consumer food wastes, wastewater biosolids, and others [12].

The results of the application of Equation A to these studies are shown in Tables S1–S36 in the Supplementary Materials, in the form of a summary of key operating conditions, with heat maps showing the difference between predicted and experimental pH values, and brief comments on interesting results or trends in each study. Selected examples are discussed below.

As can be seen from the heat maps, good agreement was found under a wide range of conditions for most or all the cases reported in the majority of these studies. In the earliest work on semi-continuous thermophilic digestion of cattle slurry in CSTR [18], the predicted pH based on $p\text{CO}_2$ matched the experimental values exactly (see Table S1). However, it should be noted that experimental pH was only recorded to one decimal place (dp) in this trial. Table 1 shows results for a study in which a thermophilic CSTR was fed on cattle manure and whey as co-substrates, with gas supplied via a hollow fibre membrane (HFM) module and H_2 input as the main variable [40]. Values of a were derived for every case (i.e., using reported average $p\text{CO}_2$ and pH from each set of conditions tested as the baseline values) and used to predict the corresponding pH in all cases. The lower part of Table 1 shows the absolute value of the difference between predicted and experimental pH. As can be seen, Equation A gave a good fit both for each phase and across all experimental conditions. Values of a based on the control reactor provided the best agreement throughout. When a coefficient derived from the highest H_2 input was used, this gave a slightly higher RMSD, possibly reflecting the small accumulation of VFA seen under these conditions. A high R^2 value across a range of conditions tested, as seen here, is not an essential indicator of good performance in all cases, since some experimental designs will show differences between different phases. Yet, where it does occur, it provides additional confidence in the predictive capacity of the equation.

Table 1. Performance of Equation A for reported average values from Luo and Angelidaki [40].

		(i)	(ii)	(iii)	(iv)	(v)	(vi)	RMSD	R ²
		No H ₂	With H ₂	No H ₂	With H ₂	No H ₂	With H ₂		
Temp	°C	55	55	55	55	55	55	-	-
OLR	g VS L ⁻¹ day ⁻¹	1.67	1.67	1.67	1.67	1.67	1.67	-	-
HRT	days	15	15	15	15	15	15	-	-
H ₂ input	L L ⁻¹ day ⁻¹	0	0.93	0	1.44	0	1.76	-	-
SMP _{tot}	L CH ₄ g ⁻¹ VS	0.275	0.407	0.271	0.478	0.287	0.515	-	-
CH ₄	%	54.2	78.4	53.1	90.2	55.4	96.1	-	-
TAN	M	n/r	n/r	n/r	n/r	n/r	n/r	-	-
VFA	M	0.002	0.004	0.002	0.012	0.002	0.038	-	-
pH	-	7.29	7.61	7.28	7.9	7.3	8.31	-	-
pCO ₂	-	0.458	0.216	0.469	0.098	0.446	0.039	-	-
<i>a</i> × 10 ⁸	-	10.41	9.81	10.42	9.81	10.43	6.99	-	-
Difference between experimental and predicted pH based on Equation A with coefficient <i>a</i> (x)									
<i>a</i> (i)	-	-	0.02	0.00	0.02	0.00	0.12	0.06	0.997
<i>a</i> (ii)	-	0.02	-	0.02	0.00	0.02	0.10	0.05	0.997
<i>a</i> (iii)	-	0.00	0.02	-	0.02	0.00	0.12	0.06	0.997
<i>a</i> (iv)	-	0.02	0.00	0.02	-	0.02	0.10	0.05	1.000
<i>a</i> (v)	-	0.00	0.02	0.00	0.02	-	0.12	0.06	0.997
<i>a</i> (vi)	-	0.16	0.13	0.16	0.12	0.16	-	0.15	1.000

n/r = not reported. Lower part of Table shows heat map with white = good, grey = reasonable, black = poor agreement.

Similar levels of agreement were found in other studies using conventional single-stage CSTR, examples are given in Tables S1–S9. Equation A also performed well where stable operation was achieved in CSTR studies with the addition of carbon monoxide (Tables S10–S12) or syngas (Tables S13 and S14). One favourable factor in some of these trials may be the absence of very low pCO₂ values due to the additional CO₂ produced from CO conversion, although CO can also be inhibitory at higher concentrations [31,41].

In 2-stage CSTR systems, good agreement was found under both mesophilic and thermophilic conditions (see, e.g., Table S15). A long-term acclimatisation study in a thermophilic 2-stage CSTR initially showed good agreement between predicted and measured pH [42]. After two years of operation, agreement appeared to deteriorate: this was likely associated with a raised VFA concentration recorded at the time, linked to the high pH and low pCO₂ value (see Table S16), and thus supports the usefulness of an equation taking VFA into account. Good agreement for comparable periods of stable operation was also found for other reactor types including AnMBR (Table S17), UASB (Table S18), AF (Table S19), and trickling filter (Table S20), and in a 2-stage system consisting of a CSTR coupled to an upflow reactor (Table S21).

Equation A also performed well when applied to pressurised systems. A 35-L mesophilic CSTR fed on wastewater biosolids was operated at four different pressures [35]: after pCO₂ was adjusted for the applied pressure, the experimental and predicted pH agreed well for all but the initial lowest pressure (Table S22). No VFA accumulation was observed that might account for this, but it is possible that other factors such as acclimatisation were involved. In a trial of pulsed H₂ addition, initial pressures were not reported but experimental and predicted pH agreed well up to a H₂/CO₂ ratio of 8 [29]; deterioration above this may have been due to changes associated with higher pressure and/or to VFA accumulation (Table S23). In another pulsed H₂ trial, initial values corrected for pressure showed good agreement [28]; other results were difficult to interpret due to uncertainty over the timing of different measurements (see Table S24a,b). Another study with headspace pressurisation [33] showed good agreement within phases, although pH was only reported to 1 dp and there was relatively little variation in pCO₂ values trial (see Table S25).

Where agreement between experimental and predicted pH values was less good, the reasons for this were often clear. One common issue was VFA accumulation. In a study of mesophilic and thermophilic digestion of cheese whey, significant swings in VFA

concentration were encountered, and various buffering strategies were adopted to control them [43]. Equation A gave only reasonable agreement, reflecting changing conditions between the different phases (Table S26). Thermophilic digestion of ensiled ryegrass was successfully achieved [44], but the VFA accumulation observed during periods of H₂ addition likely accounted for the poor agreement between predicted and experimental pH (see Table S27).

In some cases, there were apparent discrepancies in the data or results that could account for the poor agreement. In a study of mesophilic CSTR digestion of mixed sewage sludge [30], the pH in control and experimental digesters differed by 0.22 units during the start-up phase, before any H₂ addition had occurred, making comparisons with other phases problematic (Table S28). pH values also showed quite high standard deviations during this trial, perhaps reflecting the use of online measurement and/or variability between batches of feedstock. A study of mesophilic food waste digestion with pressurisation and H₂ addition used calculated pH values [37]; but these appeared to be incorrect, perhaps due to the use of acid dissociation and Henry's Law constants for 25 °C rather than for the operating temperature of 37 °C. However, when Equation A was applied 'in reverse' using baseline values from the pH calculations, it gave a much better agreement between predicted and measured pCO₂ (see Tables S29a,b).

In other cases, potential explanations remained speculative in the absence of supporting data. Digestion of ethanol distillery wastewater in a mesophilic AnMBR [55] showed poor agreement between predicted and experimental pH values in almost all conditions tested, although VFA accumulation was only seen at the highest H₂ loading (Table S30). However, the reactor was operated without sludge wastage, which could have caused changes in TAN or other unreported parameters during the experimental period.

Very few cases were found where there was no clear reason for poor agreement. In one study of a 2-stage mesophilic CSTR processing cattle manure and food waste, with H₂ injection in the second stage and gas recirculation between stages, pH reportedly fell on H₂ addition (Table S31). However, no factors accounting for this were identified [36].

In general, analysis of the data was able to demonstrate convincingly that Equation A performed very well whenever conditions were relatively stable and without major shifts in TAN or VFA concentrations; while also providing evidence to support the usefulness of an equation able to take changes in these parameters into account. Some general and methodological issues and the insights obtained from them are further discussed in Section 4.1 below.

3.2. Application of Equation B to the Literature Data

Equation B was designed to take account of the effect of digestate TAN and VFA concentrations. However, the majority of studies examined had no data on TAN and in many cases only limited details of VFA content, e.g., as total VFA without speciation or expressed in terms of Chemical Oxygen Demand (COD) or acetic acid (Hac) equivalent. Ten studies by other groups were found which had suitable data on both TAN and VFA, and these were used to compare the relative performance of the two equations.

Application of Equation B did not always show a clear improvement over Equation A, either because Equation A already gave good agreement and there was little change in VFA or TAN during the trials (see Tables S1, S3, S7 and S17), or because HCO₃⁻ and NH₄⁺ remained the main buffering pair despite the presence of VFA (Table S5); or because of other issues with the data or results (Tables S14, S22 and S28). Table 2 shows results from [46] where Equation B was able to improve estimated pH by up to 0.06 units, bringing case (iv) into the good agreement range. This and other examples of improvement can be seen in Tables S3, S4, S32 and S33. In general, the results showed that Equation B performed well, and merited further testing against datasets with more striking changes in VFA and/or TAN concentrations.

Table 2. Performance of Equations A and B for reported average values from Wahid and Horn [46].

		(i)	(ii)	(iii)	(iv)	(v)	(vi)	(vii)	RMSD	R ²
Phase		1	2	3a	3b	3c	3d	3e		
H ₂ /CO ₂		0	2	4	4	4	4	4		
Mixing	Rpm	80	80	80	120	140	170	200	-	-
Temp	°C	55	55	55	55	55	55	55	-	-
OLR	g VS L ⁻¹ day ⁻¹	3.09	2.69	2.30	2.36	2.19	2.37	2.32	-	-
HRT	Days	20	20	20	20	20	20	20	-	-
H ₂ input	L L ⁻¹ day ⁻¹	0.0	0.8	1.6	1.7	1.7	1.7	1.7	-	-
SMP total	L CH ₄ g ⁻¹ VS	0.217	0.246	0.305	0.331	0.411	0.321	0.315	-	-
CH ₄	%	62.2	37.8	31.6	38.3	40.3	41.9	40.2	-	-
TAN	M	0.10	0.11	0.13	0.15	0.14	0.14	0.14	-	-
VFA	M	0.005	0.006	0.008	0.011	0.012	0.016	0.015	-	-
pH	-	7.86	8.07	8.25	8.37	8.41	8.43	8.41	-	-
pCO ₂	-	0.378	0.207	0.137	0.124	0.119	0.116	0.120	-	-
<i>a</i> × 10 ⁸	-	2.85	2.82	2.43	1.81	1.63	1.56	1.62	-	-
<i>b</i> × 10 ⁸	-	0.255	0.277	0.278	0.233	0.193	0.162	0.171	-	-
Difference between experimental and predicted pH based on Equation A with coefficient <i>a</i> (x)										
<i>a</i> (i)	-	-	0.00	0.05	0.14	0.17	0.18	0.17	0.14	0.949
<i>a</i> (ii)	-	0.00	-	0.05	0.13	0.16	0.18	0.16	0.13	0.966
<i>a</i> (iii)	-	0.06	0.05	-	0.09	0.12	0.13	0.12	0.10	0.978
<i>a</i> (iv)	-	0.16	0.14	0.09	-	0.03	0.04	0.03	0.10	0.955
<i>a</i> (v)	-	0.19	0.17	0.12	0.03	-	0.01	0.00	0.12	0.956
<i>a</i> (vi)	-	0.21	0.19	0.13	0.04	0.01	-	0.01	0.13	0.958
<i>a</i> (vii)	-	0.19	0.18	0.12	0.03	0.00	0.01	-	0.12	0.957
Difference between experimental and predicted pH based on Equation B with coefficient <i>b</i> (x)										
<i>b</i> (i)	-	-	0.03	0.03	0.03	0.08	0.12	0.11	0.08	0.853
<i>b</i> (ii)	-	0.03	-	0.00	0.05	0.10	0.15	0.13	0.09	0.940
<i>b</i> (iii)	-	0.03	0.00	-	0.05	0.10	0.15	0.13	0.09	0.963
<i>b</i> (iv)	-	0.03	0.06	0.05	-	0.05	0.10	0.08	0.07	0.941
<i>b</i> (v)	-	0.10	0.11	0.11	0.05	-	0.05	0.03	0.08	0.929
<i>b</i> (vi)	-	0.16	0.17	0.16	0.10	0.05	-	0.01	0.12	0.947
<i>b</i> (vii)	-	0.14	0.15	0.14	0.09	0.03	0.01	-	0.11	0.942

n/r = not reported. Lower part of Table shows heat map with white = good, grey = reasonable, black = poor agreement.

3.3. Application of Equations A and B to Multi-Point Data

This part of the work was carried out to test the performance of Equations A and B with multi-point data series.

The original study that derived Equation A [6] included datasets from mesophilic CO₂ biometanisation of food waste and from a short-term study with sewage sludge. These were re-analysed to include more datapoints and provide additional information. The results are shown in Figure 1a–d, and it can be seen that Equation A performed well in both cases. For sewage sludge the correlation coefficient R² was 0.991 with n = 49 (increased from 30 in [6]), *p* < 0.000, and RMSE 0.03. For food waste digestion the equivalent values were R² = 0.880, n = 299 (increased from 242), *p* < 0.000, and RMSE 0.07 indicating that most points met the good criterion: this was despite a rise in VFA concentrations when pCO₂ briefly fell below 9% [6]. The food waste digestion study included some TAN and VFA data, and Equations A and B were also applied to points where VFA measurements were available, using interpolated TAN values where necessary. However, as TAN in this experiment was around 100 times higher than VFA on a molar basis, there was little difference between the two equations (see Figure A1 in Appendix A).

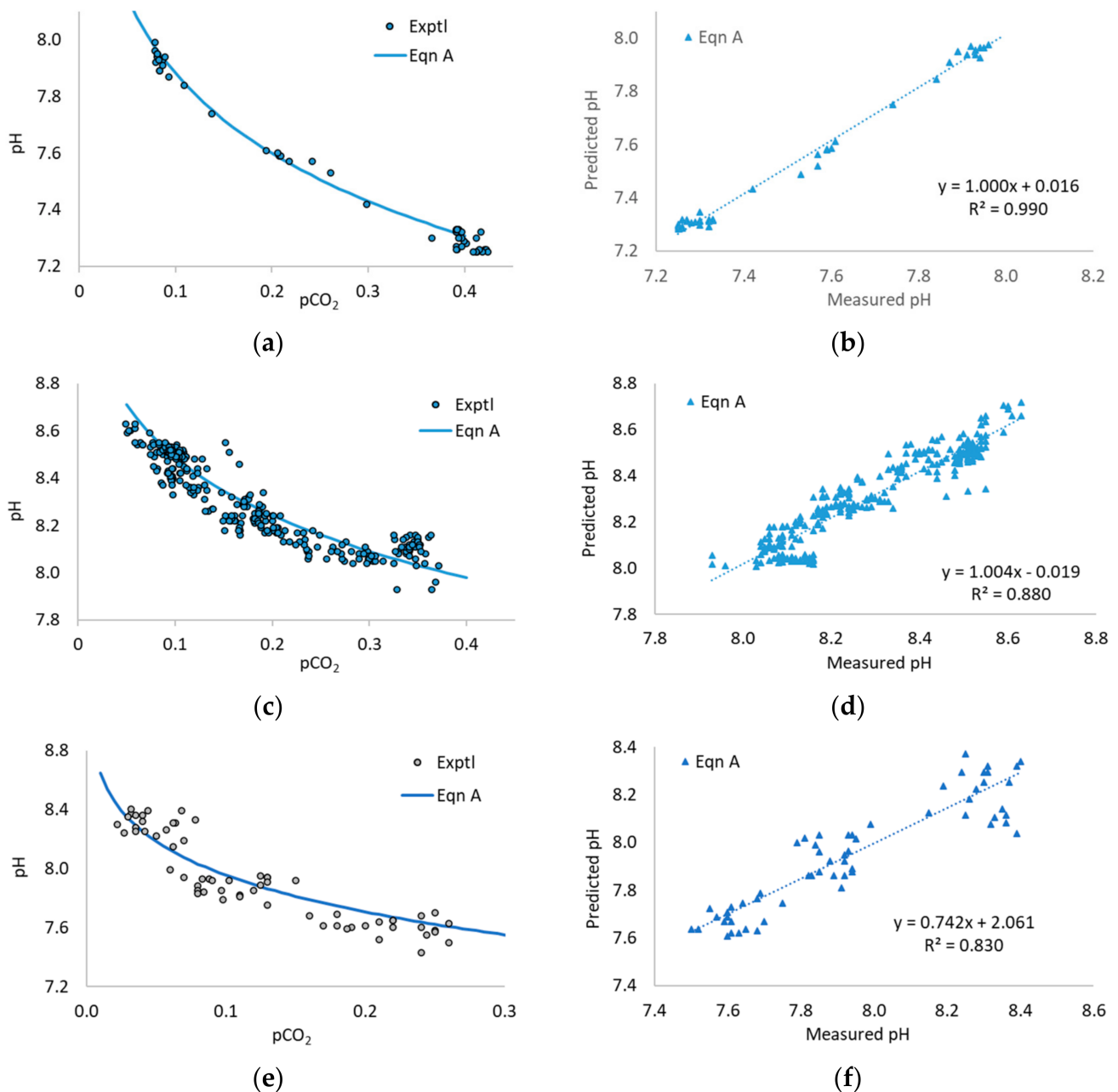


Figure 1. Experimental pCO₂ and pH values and predicted pH from Equation A for mesophilic CO₂ biomethanisation of sewage sludge (a,b) as reported in [6]; mesophilic CO₂ biomethanisation of industrial food waste (c,d) as reported in [6]; and thermophilic CO₂ biomethanisation of cattle manure (e,f) as reported in [40]. Numerical datasets were kindly provided by the authors in each case.

Several researchers kindly provided additional information in the form of experimental data series from published works [17,32,39,40,50–53]. These studies were designed to test a variety of factors, so the available data were not always ideal for the current purpose: parameters such as pH and pCO₂ were not necessarily measured frequently or on the same day [32,53], or only were reported to 1 dp [40]. Data points were sometimes unevenly distributed, with a lack of results at high, intermediate, or low pCO₂ [17,32,51]. TAN and VFA concentrations were not always monitored, and when available were usually measured less frequently than pH and pCO₂, limiting the amount of data suitable for use with Equation B. In two cases, further processing was carried out to increase the number of

data points available, by interpolation between measured $p\text{CO}_2$ values [32] and by using modelled TAN concentrations [39].

Of the eight additional datasets considered, four showed poor agreement between experimental and predicted pH values based on Equation A [17,39,50,53], in part at least for some of the reasons mentioned above. The other four showed better agreement, with R^2 values between 0.80–0.86. Figure 1e,f shows results for numerical data from the work of Luo and Angelidaki [40]: in this case Equation A gave a reasonable fit ($R^2 = 0.83$, $n = 60$, $p < 0.000$; RMSE = 0.12) for thermophilic CSTR digestion of cattle manure and whey at three H_2 loading rates across a range of $p\text{CO}_2$ values between 0.02–0.26. Results for data from mesophilic digestion of pig manure by Zhu et al. [51,52] were $R^2 = 0.85$, $n = 55$, $p < 0.000$, RMSE = 0.10; and from 2-stage mesophilic and thermophilic digestion of cattle manure by Bassani et al. [32] were $R^2 = 0.82$, $n = 32$, $p < 0.000$, RMSE = 0.10 and $R^2 = 0.869$, $n = 40$, $p < 0.000$, RMSE = 0.13, respectively. Graphs for these studies are given in Appendix A Figures A2–A6.

Four of the additional datasets included some data on TAN and VFA, but in each case, the application of Equation B was challenging. A further study on thermophilic co-digestion of cattle manure and whey by Luo and Angelidaki [17] had very few data points at high $p\text{CO}_2$ (Figure A5). TAN was measured only once in each phase, and molar VFA concentrations occasionally exceeded the average TAN value, making Equation B inapplicable for these points. In data on CO_2 biomethanisation of pig manure by Zhu et al. [50–52], Equation A had shown good results for mesophilic conditions, but TAN measurements were only available for the first part of this run (Figure A6a,b). Agreement in thermophilic conditions was poor, although there was a modest improvement in R^2 when TAN and VFA were included using Equation B (Figure A6c,d). Using VFA data and modelled TAN values from a further study on cattle manure and whey by Lovato et al. [39] also produced a slight improvement in R^2 , but in some cases, VFA concentrations exceeded the estimated TAN values, and neither Equation A nor B gave good agreement between predicted and experimental pH (see Figure A4).

Two further studies with some TAN and VFA data were available from experiments using a synthetic feedstock containing phosphates [6,23]. In one of these [23], the OLR was adjusted by changing the feed concentration and thus TAN and other parameters. Equation A gave a good correlation ($R^2 = 0.91$) between predicted and experimental pH values, but with the predicted curve offset from the experimental data (Figure 2a). Tao et al. [6] showed that a modified approach taking account of the effect of phosphate buffering could reduce this discrepancy, but it was not possible to adapt this approach for Equation B as TAN values were already used in the phosphate adjustment. However, when Equation B was applied without any phosphate correction, it also gave a considerable improvement. Figure 2a, b shows measured and predicted pH values based on Equation A, Equation B, and the phosphate adjustment for one replicate digester at OLR $3 \text{ g COD L}^{-1} \text{ day}^{-1}$. It can be seen that the phosphate adjustment increased the correlation coefficient and shifted the predicted pH closer to the experimental values, improving the RMSE from poor to good. Equation B (with no phosphate correction but adjusted for TAN and VFA) gave slightly a lower R^2 value than the phosphate adjustment, but a similar improvement in RMSE. Table 3 shows a heat map of the difference between predicted and experimental pH values using Equation A, Equation B, and the phosphate adjustment, for each phase of the experiment at OLR $3 \text{ g COD L}^{-1} \text{ day}^{-1}$. Both Equation B and the phosphate adjustment were able to reduce some discrepancies although neither were able to eliminate poor results in phase 3. Table S34 gives equivalent results for all OLR in the trial with additional statistical parameters, while Figures S2–S5 show the data series graphically: it can be seen that in general both approaches performed very well, and comparison between them can help to elucidate the relative importance of phosphate buffering, and TAN and VFA concentrations in each case.

Table 3. Cont.

OLR 3		(i)	(ii)	(iii)	(iv)	(v)	(vi)	RMSD	R ²
Difference between experimental and predicted pH based on Eqn A with coefficient $a(x)$									
$a(i)$	-	-	0.00	0.32	0.35	0.29	0.27	0.28	0.995
$a(ii)$	-	0.00	-	0.33	0.35	0.29	0.28	0.28	0.996
$a(iii)$	-	0.37	0.37	-	0.02	0.05	0.07	0.24	1.000
$a(iv)$	-	0.39	0.39	0.02	-	0.07	0.09	0.25	0.998
$a(iv)$	-	0.31	0.32	0.05	0.07	-	0.02	0.20	0.998
$a(vi)$	-	0.30	0.30	0.06	0.08	0.02	-	0.19	0.998
Difference between experimental and predicted pH based on Equation B with coefficient $b(x)$									
$b(i)$	-	-	0.01	0.13	0.14	0.06	0.00	0.09	0.980
$b(ii)$	-	0.01	-	0.14	0.15	0.07	0.01	0.10	0.979
$b(iii)$	-	0.14	0.15	-	0.01	0.07	0.13	0.11	0.983
$b(iv)$	-	0.16	0.17	0.01	-	0.09	0.15	0.13	0.990
$b(iv)$	-	0.06	0.07	0.07	0.08	-	0.06	0.07	0.987
$b(vi)$	-	0.00	0.01	0.13	0.14	0.06	-	0.09	0.997
Difference between experimental and predicted pH for Equation A with $a(x)$ and phosphate adjustment									
Period (i)	-	-	0.01	0.05	0.07	0.06	0.01	0.05	0.993
Period (ii)	-	0.01	-	0.06	0.08	0.07	0.01	0.06	0.993
Period (iii)	-	0.06	0.07	-	0.01	0.00	0.05	0.05	0.995
Period (iv)	-	0.09	0.10	0.03	-	0.02	0.07	0.07	0.996
Period (iv)	-	0.07	0.08	0.01	0.01	-	0.06	0.06	0.997
Period (vi)	-	0.01	0.02	0.04	0.06	0.05	-	0.04	0.999

n/r = not reported. Lower parts of Table show heat map with white = good, grey = reasonable, and black = poor agreement.

The second set of experiments using the same synthetic feed was carried out at controlled TAN concentrations [6]. At TAN 3 g N L⁻¹, the pH was mainly affected by ammonia, and the effect of the phosphate adjustment was small (see Supplementary Materials in [6]). The dataset of points in this experiment with measured VFA concentrations were re-analysed, using interpolated TAN values where necessary: results for 3 g N L⁻¹ are shown in Figure 2c,d. It can be seen that Equation B gave a significant improvement in fit ($R^2 = 0.919$) compared to Equation A ($R^2 = 0.702$, with $n = 54$ and $p < 0.000$ in both cases). Table S35 shows heat maps for results from Equation A using average values for each phase, while Figures S6–S9 present the data series graphically: the majority of results were in good agreement, and the two trials thus provided a powerful demonstration of the equations across a range of TAN concentrations.

It is also noteworthy that the datasets in both studies using this feedstock contained some extreme/outlying points, including values from the first days of digester operation before feeding was stabilised, and well before any H₂ addition: these correspond to points with high pCO₂ and low pH in Figure 2a,c. Thus, these results are interesting as they indicate Equation B can be used for pH prediction under a wide range of conditions, not only for the purposes of controlling H₂ addition in CO₂ biomethanisation. These two studies represent a special case, as in real organic feedstocks buffering capacity is normally provided mainly by the bicarbonate-ammonium pair. The results clearly demonstrate the value of taking VFA and TAN into consideration.

Analysis of the multi-point datasets therefore gave further clear evidence of the validity of Equation A. The additional datasets obtained from other groups did not provide a completely satisfactory demonstration of Equation B, in part because the studies considered were not designed for this purpose; although the results from these and from the data of Tao et al. [6,23] strongly indicated the potential of an equation able to take VFA and TAN into account, and confirmed the need for further experimental data.

3.4. Experimental Trial of H₂ Addition to Induce Digestion Instability

3.4.1. Digestion Performance

During the period of operation under uniform conditions between days 0–54, monitoring parameters for all digesters were in good agreement, as can be seen in Figure 3.

Average values for this period are given in column (i) of Table 4. Note that specific methane production (SMP) is expressed as total CH₄ produced per unit of organic feed VS, including any CH₄ from added H₂: on days without organic feed SMP values are omitted.

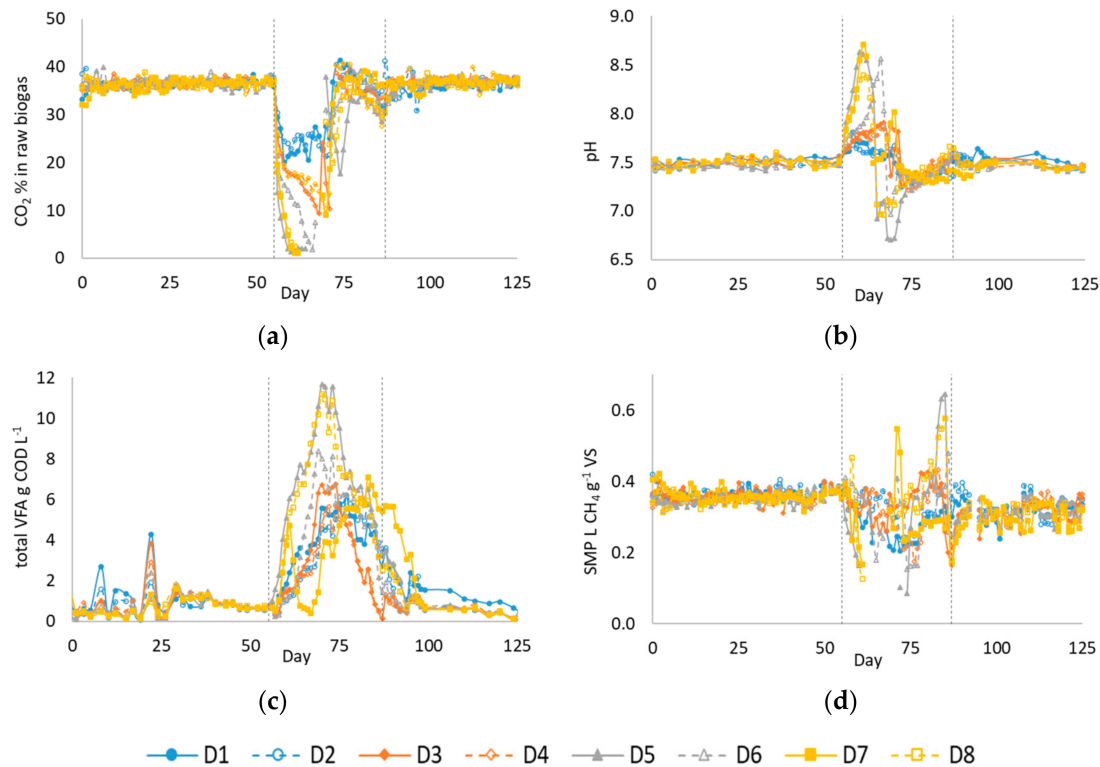


Figure 3. Values for (a) biogas CO₂ content, (b) pH, (c) total VFA, and (d) SMP in digesters D1–8 during the whole experimental period. Vertical dotted lines indicate the start of H₂ addition on day 55 and the re-establishment of full OLR in all digesters on day 87.

Table 4. Average values of monitoring parameters in D1–8 from different periods of stable operation during the experimental period.

		(i)	(ii)	(iii)	(iv)
		Before H ₂ Addition	Baseline Period 1	Baseline Period 2	After Recovery
		Day 0–54	Day 0–24	Day 25–54	Day 110–125
pH	-	7.50 ± 0.04	7.48 ± 0.04	7.50 ± 0.04	7.46 ± 0.04
TAN	M	0.131 ± 0.005	0.128 ± 0.004	0.134 ± 0.003	0.133 ± 0.004
Total VFA	M	0.008 ± 0.005	0.006 ± 0.005	0.010 ± 0.004	0.006 ± 0.003
TA	g CaCO ₃ L ⁻¹	9.38 ± 0.32	9.26 ± 0.34	9.51 ± 0.22	9.37 ± 0.28
PA	g CaCO ₃ L ⁻¹	6.33 ± 0.25	6.20 ± 0.18	6.46 ± 0.22	6.40 ± 0.23
IA	g CaCO ₃ L ⁻¹	3.05 ± 0.24	3.05 ± 0.30	3.05 ± 0.17	2.97 ± 0.15
TS	%WW	3.86 ± 0.11	3.85 ± 0.11	3.88 ± 0.12	3.88 ± 0.07
VS	%WW	2.59 ± 0.09	2.59 ± 0.08	2.58 ± 0.09	2.60 ± 0.06
SMP	L CH ₄ g ⁻¹ VS	0.358 ± 0.017	0.355 ± 0.017	0.360 ± 0.017	0.322 ± 0.027
pCH ₄	-	0.616 ± 0.008	0.617 ± 0.009	0.616 ± 0.008	0.620 ± 0.009
pCO ₂	-	0.365 ± 0.009	0.362 ± 0.010	0.367 ± 0.008	0.369 ± 0.008

Values after ± give standard deviation for data from all eight digesters.

From day 55 onwards, digesters were operated in pairs and received H₂ addition at the following rates: D1 and 2 0.81, D3 and 4 1.58, D5 and 6 2.34, and D7 and 8 2.82 L H₂ L⁻¹ day⁻¹, corresponding to a nominal 24%, 48%, 70%, and 85% of the stoichiometric H₂ requirement for conversion of CO₂ in the produced biogas and to additional COD loadings of 0.58, 1.13, 1.67,

and $2.01 \text{ g COD L}^{-1} \text{ day}^{-1}$, respectively. These rates of addition were intentionally selected to exceed the anticipated conversion capacity of the digesters in the described operating mode, especially without acclimatisation [18].

As expected, the introduction of excess H_2 led to a rapid fall in pCO_2 (Figure 3a) accompanied by a rise in pH (Figure 3b), VFA accumulation (Figure 3c), and a fall in volumetric methane production (VMP) and in SMP (Figure 3d). In D1 and 2, and D3 and 4, H_2 addition rates were maintained until day 70 apart from a brief reduction in D1 on days 65–66. However, there were clear signs of continuous VFA accumulation, along with a decline in SMP (Figure 4c,d). H_2 addition to these digesters was stopped on day 71. In D5, D7, and D8, the initial rate of H_2 addition was maintained until day 61, by which time the pH had reached 8.61, 8.71, and 8.39 with total VFA concentrations of 6.0, 4.7, and 5.4 g COD L^{-1} , respectively. Addition rates for H_2 and organic feed were varied over the next few days (details in the experimental dataset) but any signs of recovery were temporary, and H_2 addition was stopped completely on days 74, 70, and 72, respectively. D6 initially showed a slightly lower rate of pH rise and VFA accumulation than D5, and H_2 addition continued until day 66: at this point, the pH had reached 8.6 with a total VFA concentration of 5.3 g COD L^{-1} . H_2 and organic loading rates were varied over the next few days, but without lasting recovery and H_2 addition to D6 was stopped on day 71. After H_2 addition ceased pH and VFA concentrations gradually stabilised, by day 87 the full organic loading of $3.87 \text{ g VS L}^{-1} \text{ day}^{-1}$ was resumed in all digesters. The operation continued until day 125 with less frequent monitoring until the end of the period, when parameters were again measured to provide baseline values after stabilisation. Average values for this period are shown in column (iv) of Table 4 and were close to those found at the start of the trial, indicating good stabilisation.

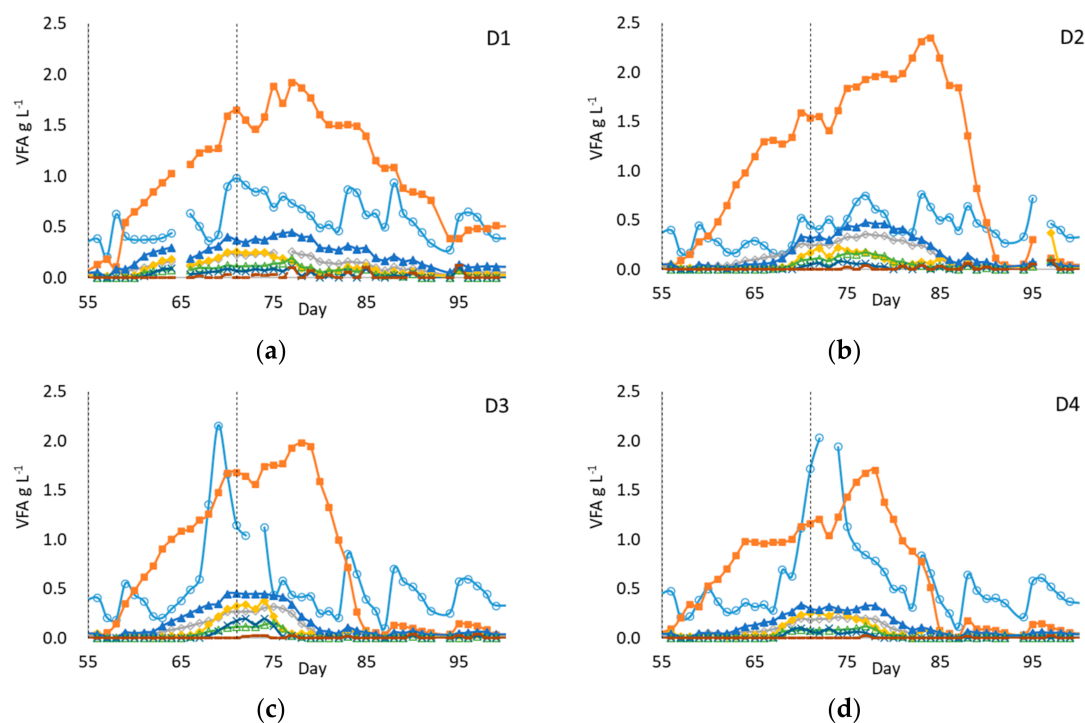


Figure 4. Cont.

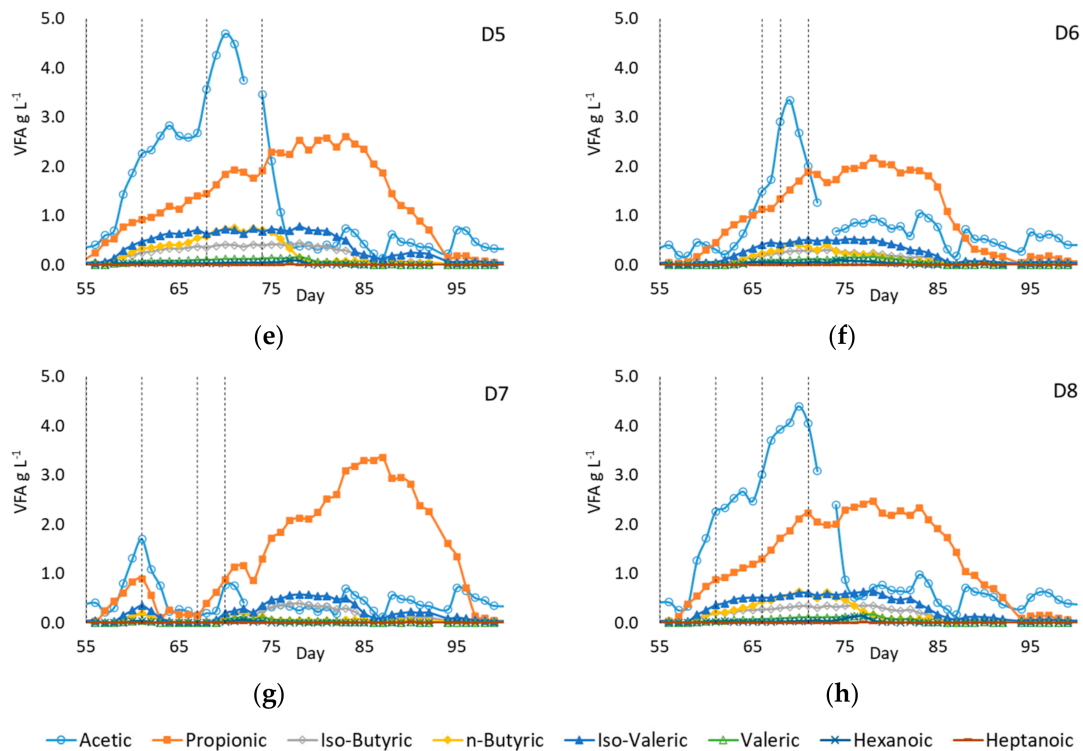


Figure 4. (a–h) VFA profiles between day 55–100 in digesters D1–8. All digesters initially received H_2 from day 55: vertical dotted lines indicate the start and end of subsequent periods of H_2 addition in each digester. Note the difference in y -axis scales for D1–4 and D5–8.

3.4.2. VFA Profiles

Figure 4 shows VFA speciation for the digesters between days 55 and 100. Following the start of H_2 injection on day 55, propionic acid accumulation occurred at similar rates in all digesters. This was expected considering the high H_2 partial pressures, which made one of the main propionate degradation pathways, to acetate, H_2 , and bicarbonate/ CO_2 , thermodynamically unfavourable [61]. The average propionate accumulation rate was $100 \text{ mg L}^{-1} \text{ day}^{-1}$ for D1–4 over the 16 days of H_2 injection, and $140 \text{ mg L}^{-1} \text{ day}^{-1}$ for D5–8 for the first 6 days of the period. Increases in acetic acid concentrations more closely reflected the difference in H_2 injection rates, with D1 and 2 apparently showing little change in acetic acid while the average rate of acetic acid accumulation in D7 and 8 during the initial six days of H_2 injection was $310 \text{ mg L}^{-1} \text{ day}^{-1}$. This is likely to have been due to homoacetogenesis occurring under high H_2 partial pressure.

During H_2 addition pH in D1–4 did not show such a marked rise as in D5–8, with measured values remaining below 7.9; whereas propionic acid concentrations continued to increase even after H_2 addition ceased. This indicated that the degradation of organic feed in D1–4 might also be blocked, although not as severely as in D5–8. Since sampling and pH measurement was conducted at the end of each daily feeding cycle, it is possible that pH values at some point during the cycle were higher than at the end, as reported in [6], and that this was responsible for the apparent blockage. This temporary unfavourable pH may also have caused partial inhibition of organic feed degradation during the 16 days of the H_2 injection period.

The VFA profile in D7 differed slightly from that in the other digesters, showing a fall in VFA concentrations when H_2 addition was paused on day 61, accompanied by a two-day gap in organic feeding followed by two days at reduced OLR. However, after OLR was restored and H_2 was reintroduced on day 67, propionate accumulation began and continued as in the other digesters even after H_2 addition ceased on day 70. Other VFA species also accumulated and then declined in all digesters in roughly the same order (see

Figure 5), with iso-valeric, n-butyric, and iso-butyric plateauing at around 0.5 g COD L⁻¹ in most case until propionate concentrations started to fall.

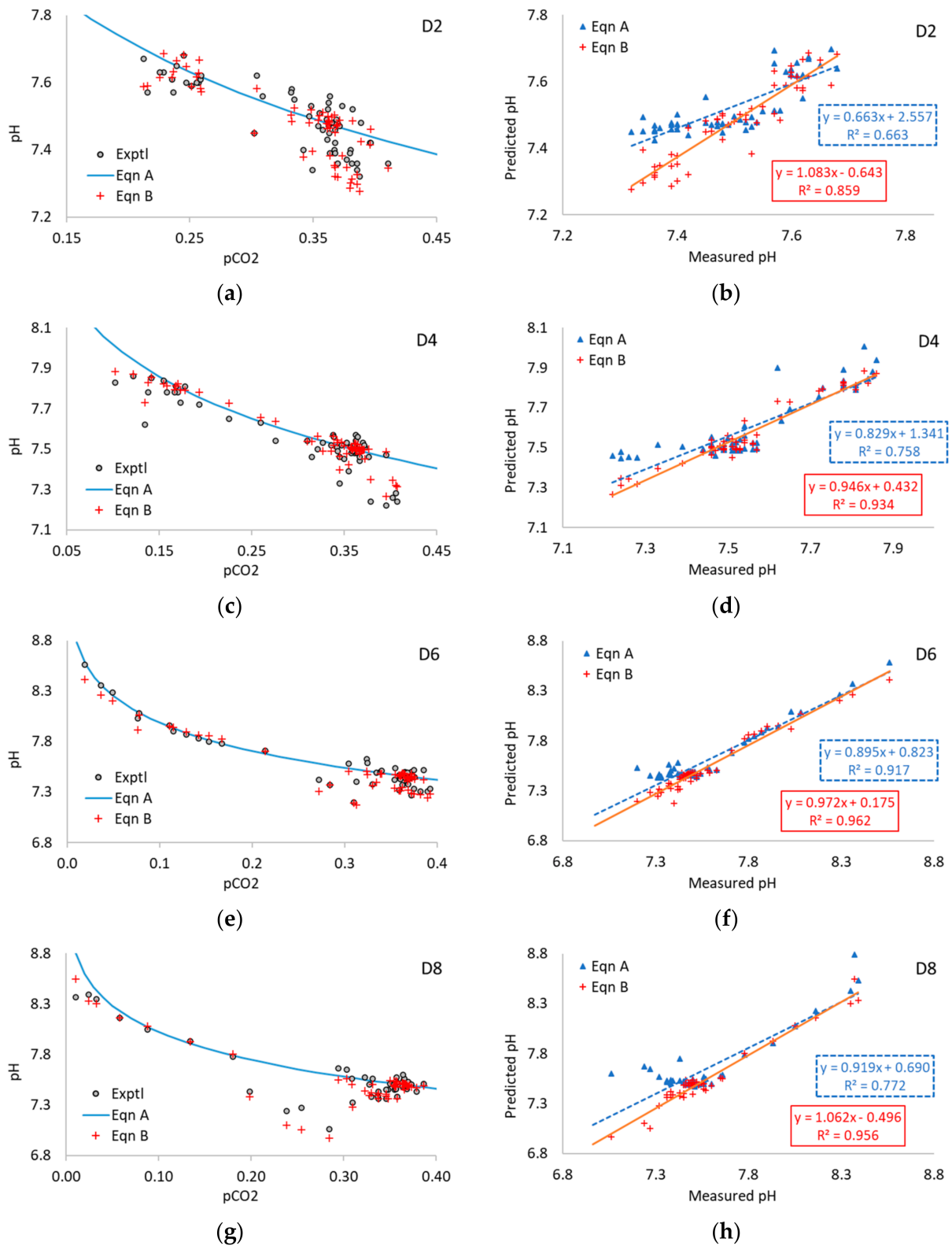


Figure 5. Experimental pCO₂ and pH values and predicted pH from Equations A and B in digesters D2 (a,b), D4 (c,d), D6 (e,f), and D8 (g,h) during mesophilic anaerobic digestion of sewage sludge at varying H₂ addition rates.

3.5. Application of Equations A and B to Experimental Data

As with the previous analysis of multi-point data series, values from the experimental work were used to evaluate the performance of Equations A and B. The dataset used consisted of points for which measured pH, pCO₂, and VFA concentrations were available, with linear interpolation of TAN values where required. Day 0–24 was initially defined as the baseline period, and average values from this (shown in column (ii) in Table 4) were used to calculate the coefficients for Equations A and B. The two equations were then applied to the data for days 25–100.

Experimental pCO₂ and pH and predicted pH values in D2, D4, D6, and D8 are shown in Figure 5, with equivalent graphs for D1, D3, D5, and D7 in Figure A7 in Appendix A. Coefficient values for Equations A and B and statistical data for all digesters are given in Table 5.

Table 5. Coefficient values and statistical parameters from the application of Equations A and B to data series from day 25–100 of experimental work.

	$a \times 10^8$	$b \times 10^8$	n	R ²		Slope		Int'cept		RMSE	
				Equation A	Equation B	Equation A	Equation B	Equation A	Equation B	Equation A	Equation B
D1	8.29	0.962	50	0.513	0.877	0.492	0.856	3.86	1.09	0.06	0.04
D2	8.85	1.052	51	0.663	0.859	0.663	1.083	2.56	−0.64	0.05	0.04
D3	8.70	1.043	51	0.774	0.937	0.915	1.000	0.68	0.02	0.08	0.04
D4	8.45	1.023	50	0.758	0.934	0.829	0.946	1.34	0.43	0.08	0.04
D5	8.87	1.103	47	0.778	0.968	0.812	0.928	1.54	0.52	0.18	0.07
D6	9.18	1.118	50	0.917	0.962	0.895	0.972	0.82	0.17	0.08	0.06
D7	8.96	1.134	46	0.950	0.973	0.935	0.967	0.54	0.21	0.07	0.06
D8	8.35	1.039	45	0.772	0.956	0.919	1.062	0.69	−0.50	0.14	0.07

Note: n = number of datapoints used (i.e., where measured values were available for pCO₂, pH, and VFA with TAN interpolated where required). Results from regression analysis were significant in all cases ($p < 0.0001$).

A fairly wide range of conditions occurred during the trial, with pCO₂ values ranging from 0.41 to 0.01, pH from 6.7 to 8.7, TAN from 1.6 to 2.1 g N L^{−1}, and VFA concentrations of up to 11.2 g COD L^{−1}. Equation A provided a good fit to the experimental data during stable operation but was less able to predict pH accurately in the period of instability during and after H₂ addition when VFA concentrations were high and varying. This resulted in poor correlation coefficients ($R^2 < 0.8$) in most cases (Table 5). In contrast, the performance of Equation B was good, with R² values ranging from 0.859 to 0.973. In comparison with Equation A, the use of Equation B gave a marked improvement in the correlation coefficient and the RMSE for experimental versus predicted data in each case and for each replicate (see Table 4). This improvement was particularly clear in D1–5 and D8, whereas in D6 and D7 Equation A also gave relatively good results. Equation B also appeared to give a slight improvement in the slope and intercept values for graphs of predicted versus experimental pH, although the difference in slope was only significant at the 5% level in D1 and D2. In all cases the RMSE value using Equation B was <0.1, indicating that it was able to provide a reliable prediction of digester pH based on pCO₂ even in periods of rapidly changing VFA content.

As a further indication of the robustness of these equations, it can be seen from Table 4 that values for a and b obtained from the baseline period were very close for all eight reactors: substitution of the relevant coefficient from another digester made only a minimal difference to the results or to the statistical parameters shown. As an additional check, values for coefficients a and b were calculated for alternative baseline periods from day 25–54, and from day 110–125 after the final stabilisation of the digesters, based on the data in columns (iii) and (iv) of Table 3. The calculated values were closely similar to those in Table 4, and use of them again had very little impact on the performance of Equations A and B. Data points between days 110–125 were not included in the analysis shown in Table 4 and Figure 5 because of a lack of measured values for TAN in the later part of the trial. Yet, inclusion of these points using interpolated TAN values also caused

only minor changes in R^2 and RMSE (details in the experimental dataset). Equation B was thus shown to be both robust and effective even in conditions of operational instability.

As noted above, in digestion of organic wastes the main buffer pair is usually HCO_3^- and NH_4^+ , with VFA^- and NH_4^+ only secondary. The strategy of excess H_2 addition was very effective in pushing up VFA concentrations to create conditions of temporary instability in the digesters for testing Equation B. While the dataset would have been strengthened by more TAN measurements in the latter part of the experimental period, the trial was thus very successful in demonstrating both the impact of short-term changes in pCO_2 and VFA on digester pH; and the potential value of Equation B as a tool for process control and management in unstable operating conditions.

4. Discussion

4.1. Methodological Issues with Data in Literature Studies

The relationship between pCO_2 and pH described in Equation A was shown to work consistently and with a high predictive capability when applied under stable operating conditions. In circumstances where changes in VFA or TAN concentrations occurred, Equation B was shown to work well both for the majority of the datasets analysed, and for the dedicated experimental work in which digester stability was tested to a point of process failure. Some results were found in data from reported studies where the equations did not give reliable results; however, it is important to try and understand why these cases occurred. The first point to note is that the analysis presented used data from all relevant published studies on in-situ CO_2 bimethanisation: it did not attempt selectively to discount datasets that did not show good agreement or to dismiss reactor types or methodologies that did not conform to typical norms. It is also important to remember that the studies considered were not specifically designed for the current purpose. As a result of these factors, there were some issues with the available data for methodological and other reasons: parameters of interest were not always measured, or not measured frequently enough, or were reported in unsuitable units, or omitting relevant details of sampling or operational conditions. Examples include experiments where H_2 was added by headspace injection (see Tables S23–S25): interpretation of data from these could be challenging, as it was not always clear whether reported pH and gas composition values were measured at the same time, while headspace pressures could have varied both between treatments and during a trial.

Many studies reported average values for a given phase or set of conditions, but these could be misleading, especially when there is considerable variation during a phase. Equation A gave poor agreement when applied to average values reported in [47]. However, if the results were recalculated using the final data points, good agreement was achieved (see Table S9). Values for individual data points may thus be preferable, while the use of data series also allows the assessment of variability.

In some studies, pH was controlled by chemical addition during some or all of the experimental period [34,48,58,62], making the data difficult or unsuitable for use in this work.

In some cases, agreement between the first and subsequent phases was poor, but improved after phase 1 (see, e.g., Tables S20, S22 and S25). This may simply reflect initial acclimatisation, especially if the first phase was short; although there is also an intriguing possibility that differences could be due to changes in gas circulation and mixing. In some studies that used gas bubblers or diffusers, there was apparently no gas recirculation in the control digester or period [23,44]; whereas there is clear evidence that changes in recirculation or mixing rates can affect performance and operating parameters [17,36,46].

Despite such issues, the available data allowed a clear demonstration of performance of the equations in each case while providing some interesting insights on practical requirements for this type of research.

4.2. General Research-Related Issues

The derivation of Equation A assumes that most baseline parameters remain applicable throughout the operating period, and changes in pH are driven primarily by pCO₂. As both the literature data and the experimental results showed, in practice this is not always so. Changes may occur over short periods, as in the current study where excess H₂ induced rapid VFA accumulation, or, as a result of longer-term processes such as washout and acclimatisation. CO₂ biomethanisation studies are often not run under the same conditions for three HRT for each phase or during start-up (see e.g., [31,49,51,60]). This is a reasonable approach where the main aim is to assess gas transfer and utilisation or changes in the microbial community, which happen on relatively rapid timescales. Yet, the stabilisation of digestate parameters can take longer and may appear as a drift in values between phases. For example, when tested on data from mesophilic cattle slurry digestion in a 140-L helically-mixed CSTR [38], Equation A gave good results (Table S8). However, there was a slight downward trend in agreement through the trial, which might have been associated with incremental shifts in TAN or VFA during acclimatisation, since the total duration for all phases was around 2.5 HRT. Unfortunately, these parameters were not reported.

Experimental design is an important factor here. Changes in baseline values during a trial due, e.g., due to acclimatisation or feedstock variability may be easy to distinguish where there is a control reactor. If TAN and/or VFA changes in the same way in both control and experimental reactors then agreement within each phase may be good, even if that between phases is not (e.g., Table S25). However, the identification of such changes is more difficult when different conditions are run in series without controls.

There may also be specific reasons for differences in TAN between control and experimental digesters within a phase, such as changes in microbial biomass associated with growth in the hydrogenotrophic methanogenic population during in situ CO₂ biomethanisation [23], or toxicity effects from syngas or other inhibitors. These effects may help to explain patterns where agreement across several phases is good for control reactors but poor for experimental ones (e.g., Table S36). In such cases, results from control digesters do not resolve the problem, although it may still be possible to observe trends in the results.

The original studies by Luo et al. [17,18,40,41] were run with control reactors, at relatively short HRTs of 15 days, in conditions that allowed steady stable operation, and therefore produced good agreement in all cases: see Tables S1, S2, S3 and S10. Studies of this type can give high R² values for prediction across multiple conditions but, as noted earlier, this is not a requirement for demonstrating the good performance of the equations tested if there are other reasons for variability across phases.

Several of the above examples add further support to the practical value of an equation that can deal with changes over both long and short timescales. The present work demonstrated that Equation B was able to deal with acute short-term changes, such as the rapid VFA accumulation in the current trial. It could also accommodate longer-term changes and shifts in TAN: the evidence for this is slightly more tentative due to the relative scarcity of datasets with TAN measurements but can be seen, e.g., in Tables S7, S22, S34 and S35. Equation B also performed well when there were changes in both TAN and VFA (e.g., Tables S4 and S32). As noted above, Equation B is thus applicable in cases where pH is affected by other factors in addition to changes in pCO₂ induced by CO₂ biomethanisation.

4.3. Considerations for Large-Scale Operation

In this work pCO₂ values from literature and experimental data were used to predict pH, and the results were then compared with reported pH values. pH was selected as the output because this is widely used as an indicator of stability in day-to-day operation. However, the same relationships can of course be used to predict pCO₂ from pH, and monitoring of either parameter in conjunction with the use of these equations could thus provide a useful basis for process control in CO₂ biomethanisation.

Equation A allows calculation of pH values from two parameters (digester temperature and pCO₂), with a further two (TAN and VFA) required for Equation B. Calibration can

be achieved by measurement of these parameters under one set of conditions, which does not necessarily have to be baseline operation (e.g., without H₂ addition in the case of CO₂ biomethanisation), as long as these are representative of a stable operating mode. In contrast, alternative models to predict pH such as ADM1 [63] generally require a large number of input values for calibration. These more complex models also predict many other performance and stability parameters, but their use in real-time control is still uncommon, although interest in this application is expanding [20,22].

Variations in the feedstock can cause changes in total Kjeldahl nitrogen and TAN, and while these can be controlled in laboratory experiments they also affect commercial AD plants [20]. Even with relatively consistent feedstocks such as sewage sludges, biosolids concentration may vary over time as a result, e.g., of changes in dewatering practices. AD operators at WWTW can accommodate this by changing the applied OLR or HRT if required, but TAN concentrations will still vary and may affect the ammonium-bicarbonate equilibrium, pCO₂ and pH and thus the coefficients for Equation A and B. At commercial sites with a single digester, operation without a 'control' reactor represents the normal situation: these sites may also have less staff time available for digester management, so simple robust process control systems for CO₂ biomethanisation are likely to be particularly valuable in this case [21]. At multi-digester sites it may be possible to process all of the biogas generated on the site in one digester retrofitted for CO₂ biomethanisation [6]; in this case the performance of other digesters could provide control data indicating any changes due, e.g., to feedstock variation.

Use of a relationship which takes account of the effect of changes in TAN and VFA concentrations may appear to require increased monitoring compared to current practice at many AD plants [27]. However, as noted earlier, the objective in full-scale operation is normally to remain within an envelope of safe operating conditions. As Equations A and B are equivalent when no VFA is present, Equation A can be used when conditions are stable. Analysis for TAN and VFA is relatively straightforward, and in normal circumstances TAN values do not change very rapidly. Monitoring of additional parameters can therefore be performed infrequently or not at all when an operation is stable, and introduced or stepped up only if some disturbance makes this necessary, meaning the requirement for more parameters need not be burdensome [21].

No detailed analysis was made to compare the values of coefficients *a* or *b* derived for different sets of feedstocks or operating conditions. However, it is interesting to note that four studies on thermophilic (55 °C) CSTR digestion of cattle manure obtained from three different sources gave values for *a* of around $2\text{--}3 \times 10^{-8}$ when operating stably (Tables S1, S15, S16 and S32); values for mesophilic (37 and 40 °C) operation were slightly higher at around $5\text{--}6 \times 10^{-8}$ (Tables S8 and S15). Three independent studies of sewage sludge digestion in mesophilic (37 °C) CSTR gave *a* values of $11\text{--}15 \times 10^{-8}$ (Tables S6, S10 and S38). Crop and agro-wastes and food waste feedstocks, as defined in [12], were more diverse, forestalling any direct comparison. These different values of *a* reflect both the digestate TAN concentration, and the effect of other physico-chemical characteristics of the digestate on the Henry's and acid disassociation constants; when the VFA concentration is zero, *b* is simply equal to *a* divided by the molar TAN concentration. While it is easy to obtain values for *a* or *b* from any suitable set of baseline parameters for a given digester, the idea that there may be typical values of these coefficients which could be applied generally and/or that can be linked to other digestate properties is of interest and worth consideration in further work

5. Conclusions

In the current work, the performance of the two equations was well demonstrated across a wide range of operating conditions and data sources.

Equation A provides a relationship between two simple parameters, often routinely measured, which showed good agreement with experimental data when applied under

stable operating conditions. This approach therefore appears suitable as a basis for control of H₂ addition in CO₂ biomethanisation of organic substrates.

Equation A performed less well for digesters undergoing dynamic change or experiencing instability, as indicated, e.g., by VFA accumulation. In these situations, the use of Equation B incorporating VFA and TAN concentrations was generally able to improve prediction, giving RMSD values of <0.1 pH units: this was clearly demonstrated by experimental work in which unstable conditions were deliberately induced to test the equations' performance. Both TAN and VFA are relatively straightforward to monitor and when they are included along with pCO₂ as in the derived Equation B, the range of application can be extended from stable operation to cover both dynamic change, and crisis management and recovery if digester operation becomes unstable.

As both Equation A and B are derived from fundamental principles, the discrepancies that are seen in some cases between predicted and experimental data most likely reflect limitations in typical measurement accuracy and/or experimental design. This and the fact that the equations performed well when applied to data from a wide range of plant configurations and substrates gives strong support to the view that they are suitable for application on real-world operational sites.

Establishing the required coefficient values for each equation is a simple process requiring only basic data from a period of stable operation. Once these are determined for a particular waste/digester combination, the use of this approach offers a reliable means of optimising the biomethanisation potential of a plant without the risk of exceeding critical values for pH or pCO₂. This should provide the industry with the confidence to adopt this emerging biotechnology, which could significantly increase the efficiency of utilisation of carbon from organic substrates. The research thus further strengthens the case for promoting in situ CO₂ biomethanisation as a means of maximising the value of existing infrastructure and resources in the waste and agri-food sectors.

Supplementary Materials: The following supporting information can be downloaded at: <https://www.mdpi.com/article/10.3390/pr11010113/s1>. [64,65].

Author Contributions: Development of equations, Y.Z.; Conceptualisation of study, C.J.B., Y.Z. and S.H.; literature review and data analysis, S.H. and Y.Z.; supervision of experimental work, C.J.B., S.H. and Y.Z.; analysis of experimental data: Y.Z. and S.H.; writing—original draft preparation, S.H.; writing—review and editing, Y.Z. and C.J.B.; funding acquisition, C.J.B., S.H. and Y.Z. All authors have read and agreed to the published version of the manuscript.

Funding: This research was supported by the IBCat H2AD project (EP/M028208/1) funded by the Engineering and Physical Sciences Research Council (EPSRC). The APC were funded by MDPI Topic Anaerobic Digestion Processes.

Data Availability Statement: The experimental data in this study are openly available in <https://doi.org/10.5258/SOTON/D2488>. For other data requests please contact the corresponding authors.

Acknowledgments: The authors would like to thank the following for the provision of additional numerical datasets: Ilaria Bassani, Istituto Italiano di Tecnologia, Genova, Italy; Giovanna Lovato, Instituto Mauá de Tecnologia, São Caetano do Sul, Brazil; Gang Luo, Department of Environmental Science and Engineering, Fudan University, Shanghai, China; Bing Tao, formerly of the University of Southampton, Southampton, UK; Xianpu Zhu, Shanghai Jiao Tong University, Shanghai, China. The authors also gratefully acknowledge the help and support of the Specialist Technical Staff of the Environmental Laboratories at the University of Southampton, UK.

Conflicts of Interest: The authors declare no conflict of interest. The funders had no role in the design of the study, namely in the collection, analyses, or interpretation of data; in the writing of the manuscript; or in the decision to publish the results.

Appendix A

Figures A1–A7 show results for the application of Equation A and where possible Equation B to datasets associated with [6,17,32,39,40,50–53], and with the experimental

work in the current trial. Numerical datasets associated with the published literature were kindly provided by the authors in each case. Note that graphs do not include baseline values used for deriving coefficients a and b .

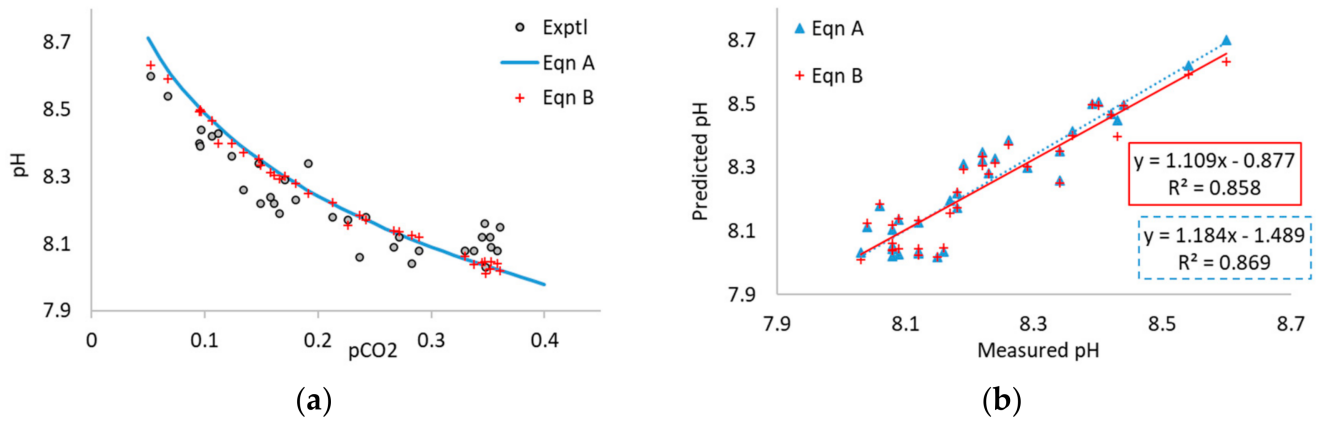


Figure A1. (a) Measured pCO₂ and measured and predicted pH values and (b) predicted pH values from Equations A and B for mesophilic CO₂ biomethanisation of industrial food waste for points with measured VFA and measured or interpolated TAN associated with Tao et al. [6]. See Figure 1c,d in the main text for results from Equation A for the full dataset, and Table S5 for operating conditions and average results for each phase.

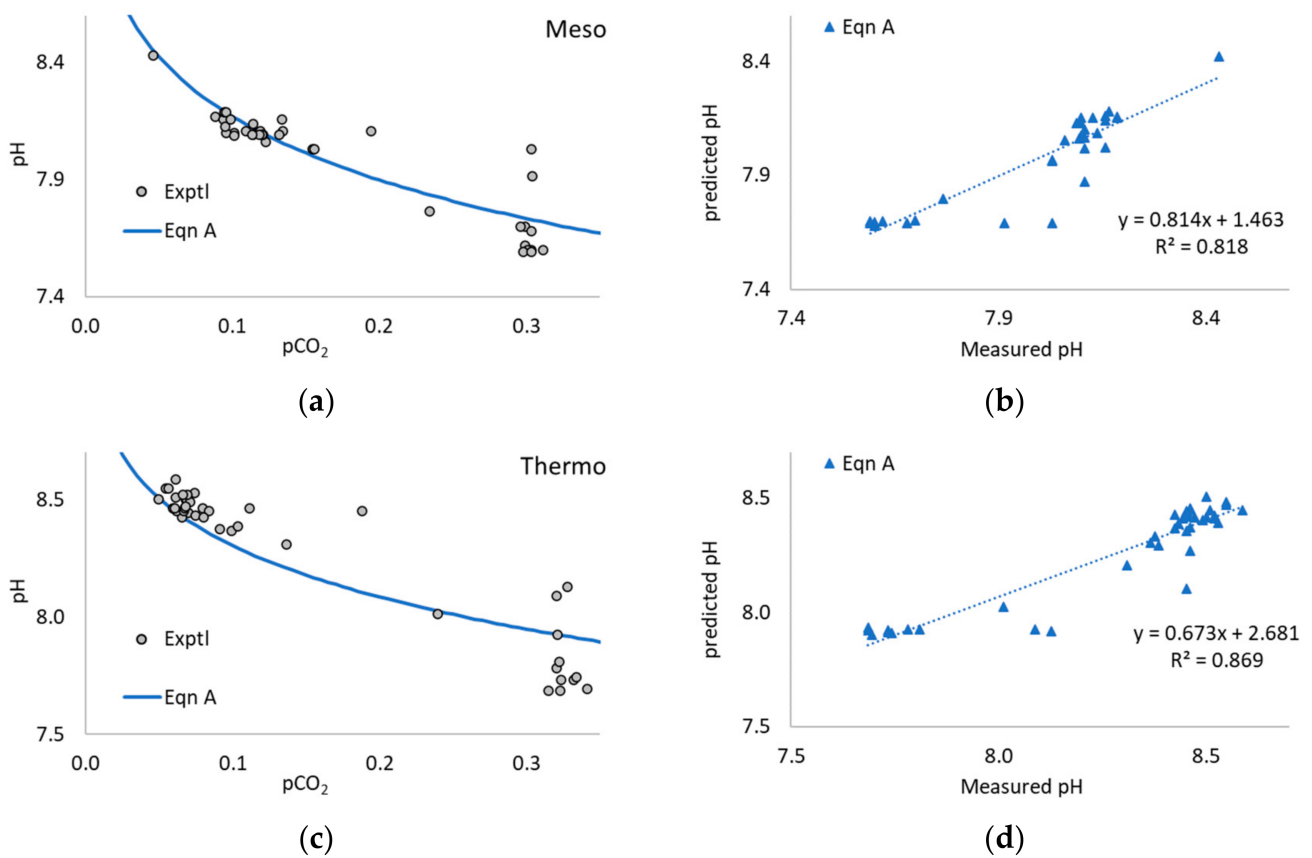


Figure A2. Experimental pCO₂ and pH values and predicted pH from Equation A for 2-stage mesophilic (a,b) and thermophilic (c,d) CO₂ biomethanisation of cattle manure associated with Bassani et al. [32]. See Table S15 for operating conditions and average results for each phase.

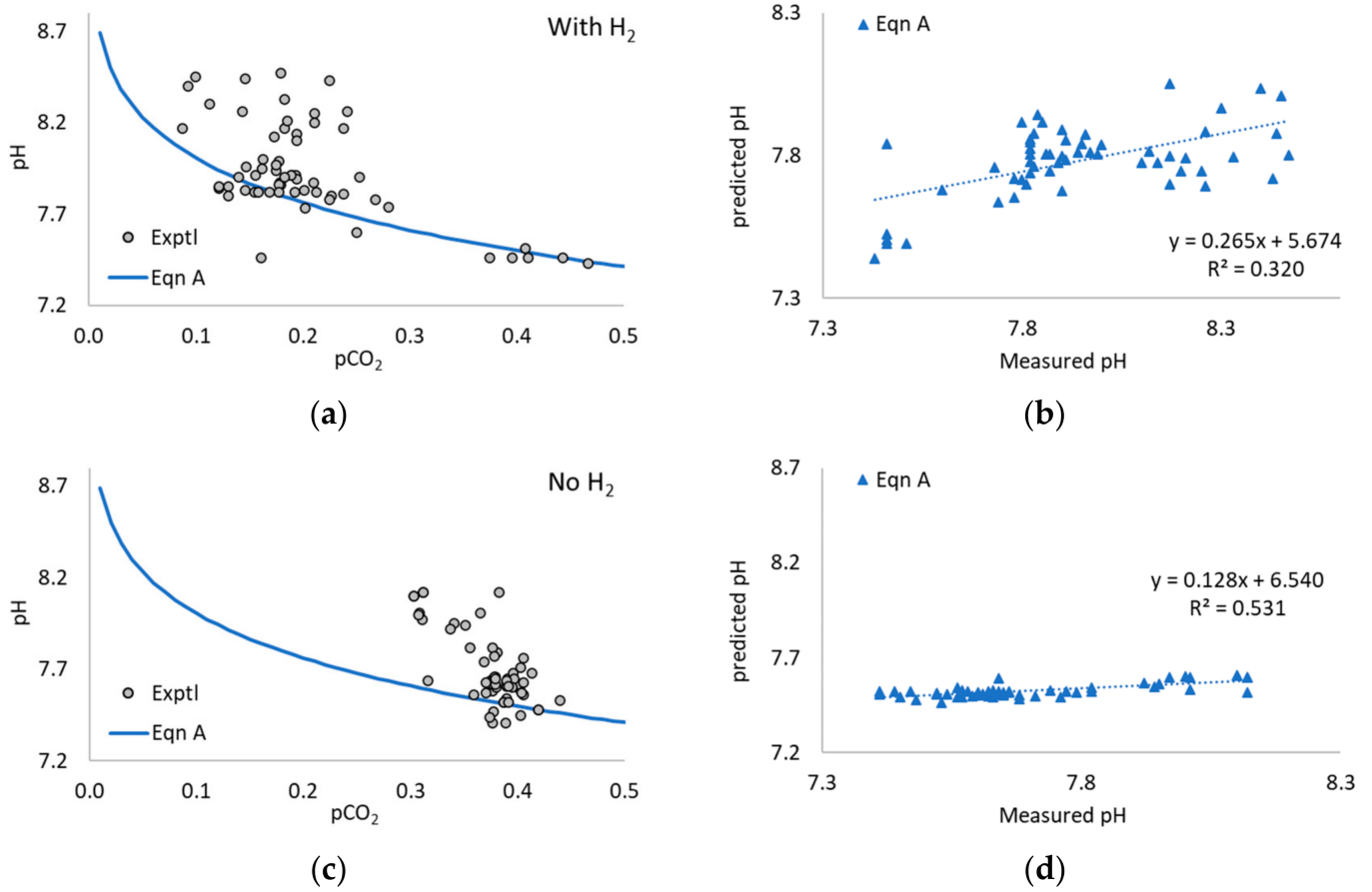


Figure A3. Experimental pCO₂ and pH values and predicted pH from Equation A for thermophilic UASB fed on potato starch wastewater with (a,b) and without (c,d) H₂ addition associated with Bassani et al. [53]. See Table S18 for operating conditions and average results for each phase.

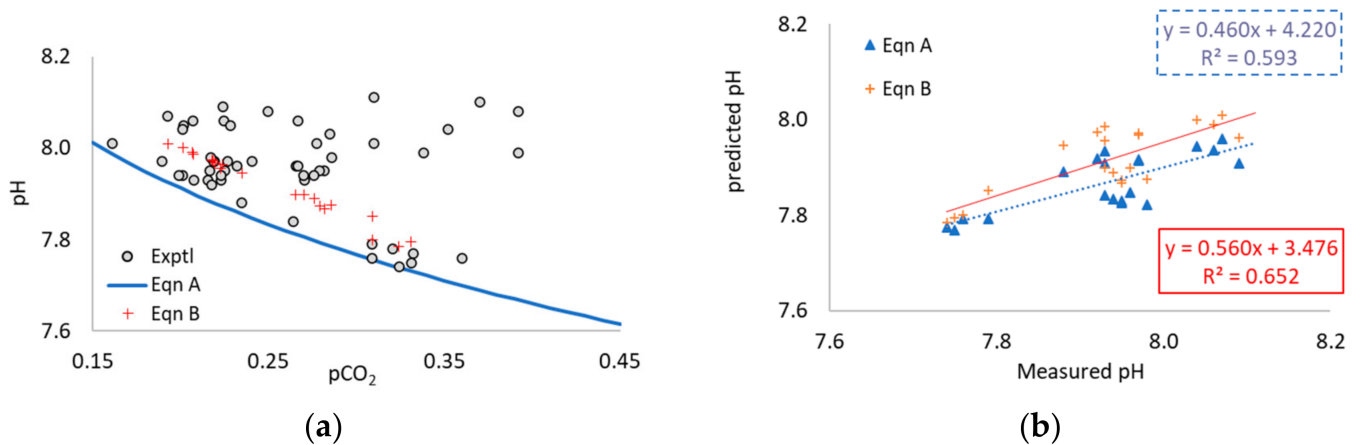


Figure A4. (a) Measured pCO₂ and measured and predicted pH values and (b) predicted pH values from Equations A and B for thermophilic CO₂ biometanisation of cattle manure and whey using modelled TAN values associated with Lovato et al. [39]. See Table S7 for operating conditions and average results for each phase.

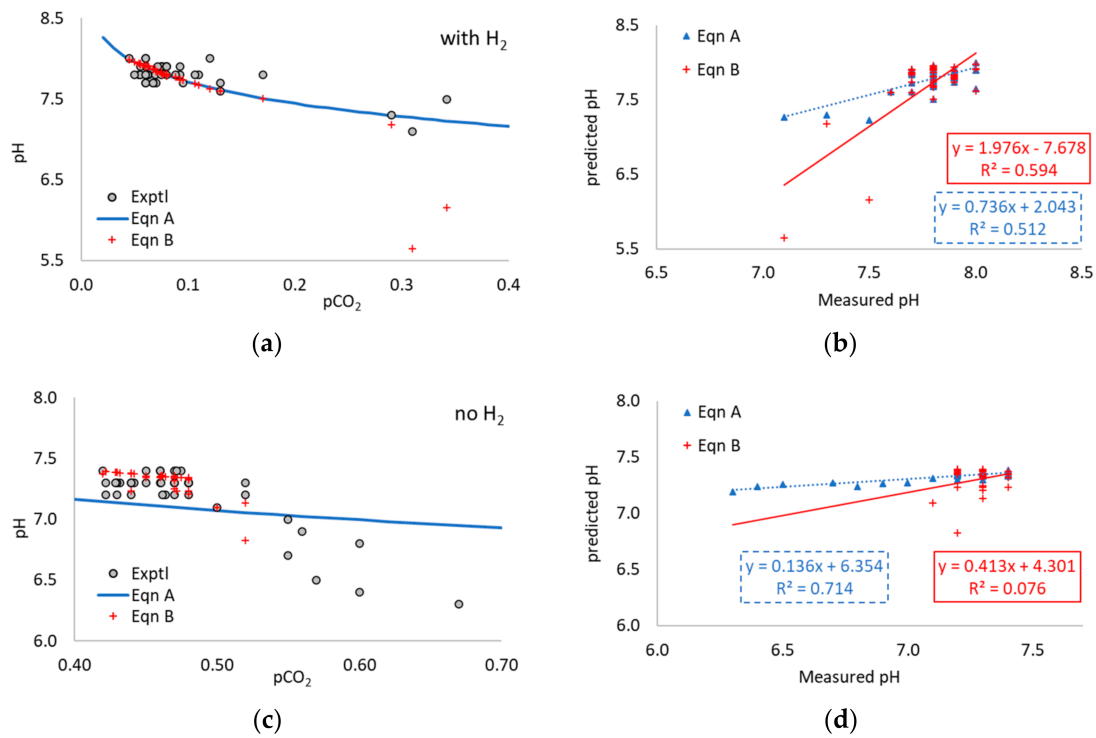


Figure A5. Experimental pCO₂ and pH values and predicted pH from Equations A and B for thermophilic CO₂ biomethanisation of cattle manure and whey with (a,b) and without (c,d) H₂ addition associated with Luo and Angelidaki [17]. See Table S3 for operating conditions and average results for each phase.

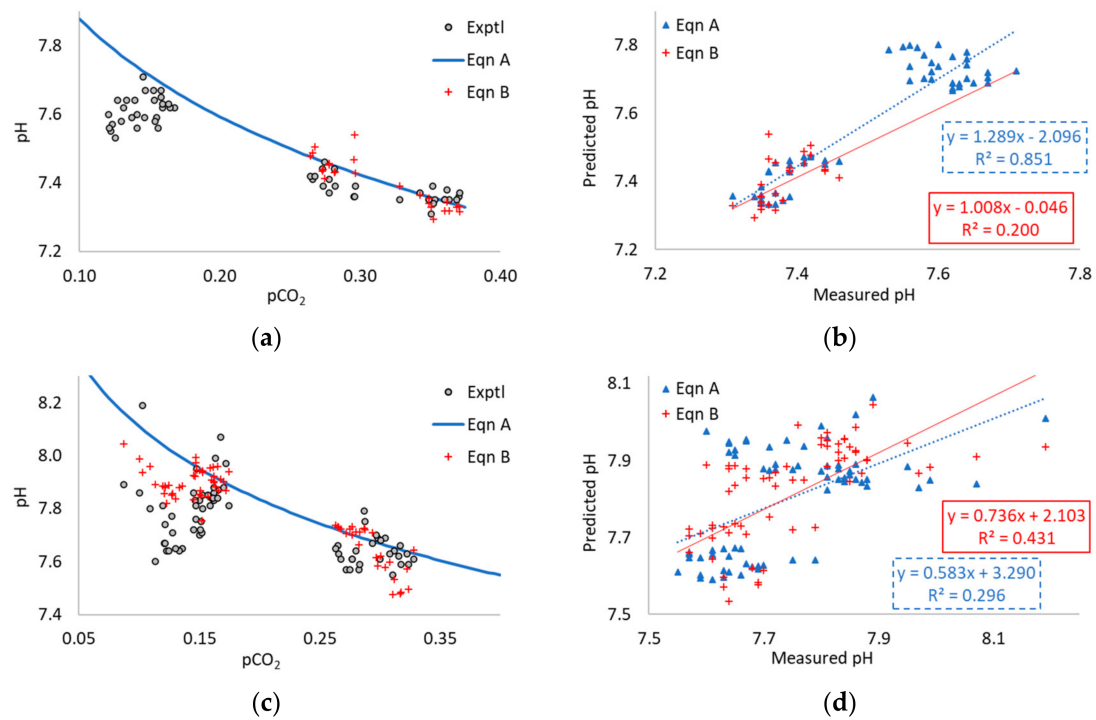


Figure A6. Experimental pCO₂ and pH values and predicted pH from Equation A for mesophilic (a,b) and thermophilic (c,d) CO₂ biomethanisation of pig manure associated with Zhu et al. [50–52]. See Table S4 for operating conditions and average results for each phase.

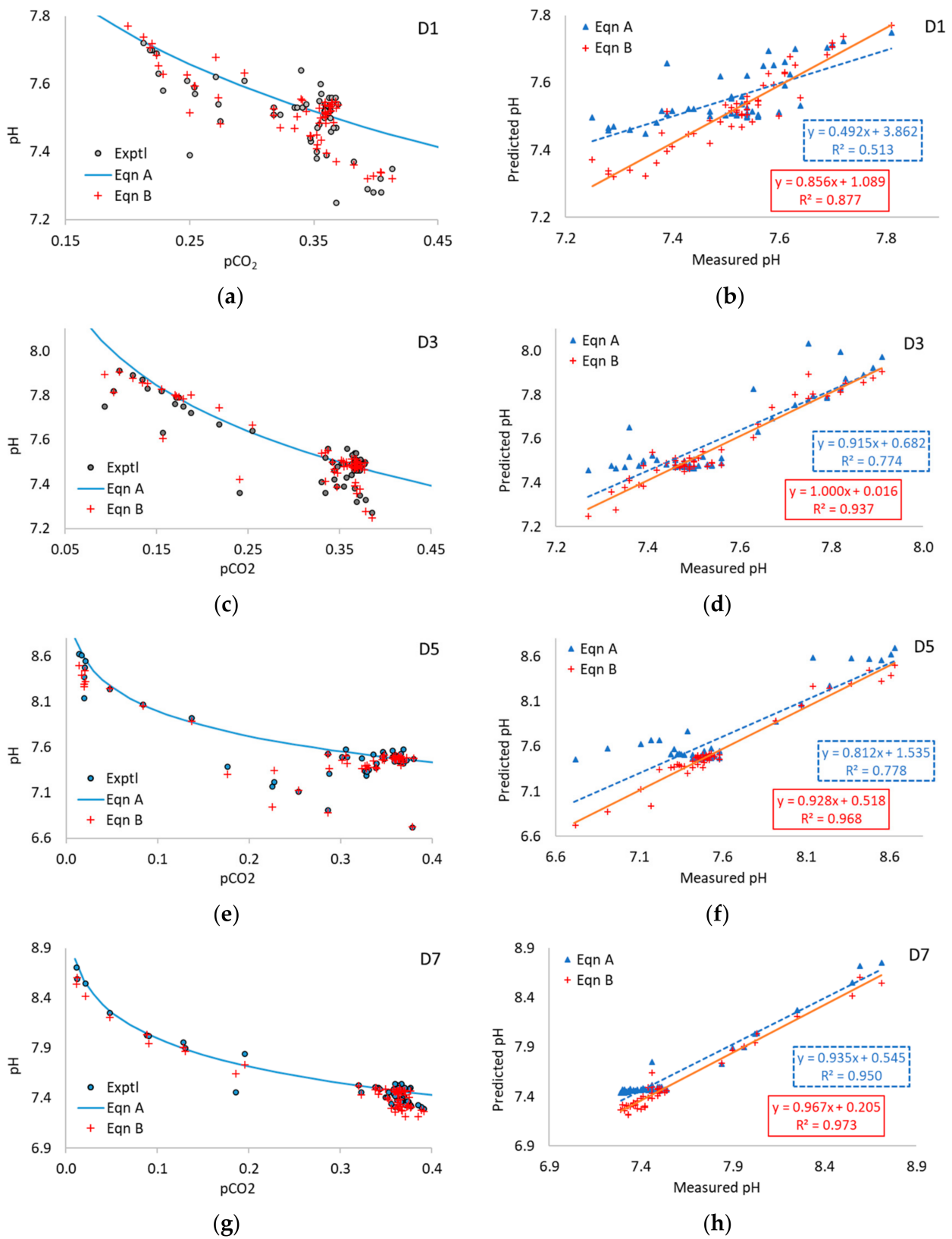


Figure A7. Experimental pCO₂ and pH values and predicted pH from Equations A and B in digesters D1 (a,b), D3 (c,d), D5 (e,f), and D7 (g,h) during mesophilic anaerobic digestion of sewage sludge at varying H₂ addition rates. For even-number digesters, see Figure 5 in the main text.

References

1. Zeikus, J. The biology of methanogenic bacteria. *Bacteriol. Rev.* **1977**, *41*, 514–541. [[CrossRef](#)] [[PubMed](#)]
2. Luo, G.; Angelidaki, I. Integrated biogas upgrading and hydrogen utilization in an anaerobic reactor containing enriched hydrogenotrophic methanogenic culture. *Biotechnol. Bioeng.* **2012**, *109*, 2729–2736. [[CrossRef](#)] [[PubMed](#)]
3. Rafrafi, Y.; Laguillaumie, L.; Dumas, C. Biological Methanation of H₂ and CO₂ with Mixed Cultures: Current Advances, Hurdles and Challenges. *Waste Biomass Valorization* **2020**, *12*, 5259–5282. [[CrossRef](#)]
4. Zavarkó, M.; Imre, A.R.; Pörzse, G.; Csedő, Z. Past, Present and Near Future: An Overview of Closed, Running and Planned Biomethanation Facilities in Europe. *Energies* **2021**, *14*, 5591. [[CrossRef](#)]
5. Aryal, N.; Kvist, T.; Ammam, F.; Pant, D.; Ottosen, L.D. An overview of microbial biogas enrichment. *Bioresour. Technol.* **2018**, *264*, 359–369. [[CrossRef](#)]
6. Tao, B.; Zhang, Y.; Heaven, S.; Banks, C.J. Predicting pH rise as a control measure for integration of CO₂ biomethanisation with anaerobic digestion. *Appl. Energy* **2020**, *277*, 115535. [[CrossRef](#)]
7. Andreides, D.; Stransky, D.; Bartackova, J.; Pokorna, D.; Zabranska, J. Syngas biomethanation in countercurrent flow trickle-bed reactor operated under different temperature conditions. *Renew. Energy* **2022**, *199*, 1329–1335. [[CrossRef](#)]
8. Ghofrani-Isfahani, P.; Tsapekos, P.; Peprah, M.; Kougiyas, P.; Zervas, A.; Zhu, X.; Yang, Z.; Jacobsen, C.S.; Angelidaki, I. Ex-Situ biogas upgrading in thermophilic trickle bed reactors packed with micro-porous packing materials. *Chemosphere* **2022**, *296*, 133987. [[CrossRef](#)]
9. Paniagua, S.; Lebrero, R.; Muñoz, R. Syngas biomethanation: Current state and future perspectives. *Bioresour. Technol.* **2022**, *358*, 127436. [[CrossRef](#)]
10. Dong, D.; Choi, O.K.; Lee, J.W. Influence of the continuous addition of zero valent iron (ZVI) and nano-scaled zero valent iron (nZVI) on the anaerobic biomethanation of carbon dioxide. *Chem. Eng. J.* **2022**, *430*, 132233. [[CrossRef](#)]
11. Geppert, F.; Liu, D.; van Eerten-Jansen, M.; Weidner, E.; Buisman, C.; Ter Heijne, A. Bioelectrochemical power-to-gas: State of the art and future perspectives. *Trends Biotechnol.* **2016**, *34*, 879–894. [[CrossRef](#)]
12. Bywater, A.; Heaven, S.; Zhang, Y.; Banks, C.J. Potential for Biomethanisation of CO₂ from Anaerobic Digestion of Organic Wastes in the United Kingdom. *Processes* **2022**, *10*, 1202. [[CrossRef](#)]
13. D’Silva, T.C.; Isha, A.; Chandra, R.; Vijay, V.K.; Subbarao, P.M.V.; Kumar, R.; Chaudhary, V.P.; Singh, H.; Khan, A.A.; Tyagi, V.K. Enhancing methane production in anaerobic digestion through hydrogen assisted pathways—A state-of-the-art review. *Renew. Sustain. Energy Rev.* **2021**, *151*, 111536. [[CrossRef](#)]
14. Lai, C.S.; McCulloch, M.D. Sizing of stand-alone solar PV and storage system with anaerobic digestion biogas power plants. *IEEE Trans. Ind. Electron.* **2016**, *64*, 2112–2121. [[CrossRef](#)]
15. Wang, P.; Wang, J.; Jin, R.; Li, G.; Zhou, M.; Xia, Q. Integrating biogas in regional energy systems to achieve near-zero carbon emissions. *Appl. Energy* **2022**, *322*, 119515. [[CrossRef](#)]
16. Angelidaki, I.; Treu, L.; Tsapekos, P.; Luo, G.; Campanaro, S.; Wenzel, H.; Kougiyas, P.G. Biogas upgrading and utilization: Current status and perspectives. *Biotechnol. Adv.* **2018**, *36*, 452–466. [[CrossRef](#)]
17. Luo, G.; Angelidaki, I. Co-digestion of manure and whey for in situ biogas upgrading by the addition of H₂: Process performance and microbial insights. *Appl. Microbiol. Biotechnol.* **2013**, *97*, 1373–1381. [[CrossRef](#)]
18. Luo, G.; Johansson, S.; Boe, K.; Xie, L.; Zhou, Q.; Angelidaki, I. Simultaneous hydrogen utilization and in situ biogas upgrading in an anaerobic reactor. *Biotechnol. Bioeng.* **2012**, *109*, 1088–1094. [[CrossRef](#)]
19. Drog, B. *Process Monitoring in Biogas Plants*; IEA Bioenergy: Paris, France, 2013.
20. Gaida, D.; Wolf, C.; Bongards, M. Feed control of anaerobic digestion processes for renewable energy production: A review. *Renew. Sustain. Energy Rev.* **2017**, *68*, 869–875. [[CrossRef](#)]
21. Nguyen, D.; Gadhamshetty, V.; Nitayavardhana, S.; Khanal, S.K. Automatic process control in anaerobic digestion technology: A critical review. *Bioresour. Technol.* **2015**, *193*, 513–522. [[CrossRef](#)]
22. Wade, M.J. Not just numbers: Mathematical modelling and its contribution to anaerobic digestion processes. *Processes* **2020**, *8*, 888. [[CrossRef](#)]
23. Tao, B.; Alessi, A.M.; Zhang, Y.; Chong, J.P.; Heaven, S.; Banks, C.J. Simultaneous biomethanisation of endogenous and imported CO₂ in organically loaded anaerobic digesters. *Appl. Energy* **2019**, *247*, 670–681. [[CrossRef](#)]
24. APHA. *Standard Methods for the Examination of Water and Wastewater*; American Public Health Association: Washington, DC, USA, 2005.
25. Ripley, L.E.; Boyle, W.C.; Converse, J.C. Improved alkalimetric monitoring for anaerobic digestion of high-strength wastes. *J. (Water Pollut. Control Fed.)* **1986**, *58*, 406–411.
26. Walker, M.; Zhang, Y.; Heaven, S.; Banks, C. Potential errors in the quantitative evaluation of biogas production in anaerobic digestion processes. *Bioresour. Technol.* **2009**, *100*, 6339–6346. [[CrossRef](#)] [[PubMed](#)]
27. Wu, D.; Li, L.; Zhao, X.; Peng, Y.; Yang, P.; Peng, X. Anaerobic digestion: A review on process monitoring. *Renew. Sustain. Energy Rev.* **2019**, *103*, 1–12. [[CrossRef](#)]
28. Agneessens, L.M.; Ottosen, L.D.M.; Andersen, M.; Olesen, C.B.; Feilberg, A.; Kofoed, M.V.W. Parameters affecting acetate concentrations during in-situ biological hydrogen methanation. *Bioresour. Technol.* **2018**, *258*, 33–40. [[CrossRef](#)] [[PubMed](#)]
29. Agneessens, L.M.; Ottosen, L.D.M.; Voigt, N.V.; Nielsen, J.L.; de Jonge, N.; Fischer, C.H.; Kofoed, M.V.W. In-situ biogas upgrading with pulse H₂ additions: The relevance of methanogen adaption and inorganic carbon level. *Bioresour. Technol.* **2017**, *233*, 256–263. [[CrossRef](#)] [[PubMed](#)]
30. Alfaro, N.; Fdz-Polanco, M.; Fdz-Polanco, F.; Díaz, I. H₂ addition through a submerged membrane for in-situ biogas upgrading in the anaerobic digestion of sewage sludge. *Bioresour. Technol.* **2019**, *280*, 1–8. [[CrossRef](#)]

31. Andreides, D.; Pokorna, D.; Zabranska, J. Assessing the syngas biomethanation in anaerobic sludge digestion under different syngas loading rates and homogenisation. *Fuel* **2022**, *320*, 123929. [[CrossRef](#)]
32. Bassani, I.; Kougiyas, P.G.; Treu, L.; Angelidaki, I. Biogas upgrading via hydrogenotrophic methanogenesis in two-stage continuous stirred tank reactors at mesophilic and thermophilic conditions. *Environ. Sci. Technol.* **2015**, *49*, 12585–12593. [[CrossRef](#)]
33. Corbellini, V.; Catenacci, A.; Malpei, F. Hydrogenotrophic biogas upgrading integrated into WWTPs: Enrichment strategy. *Water Sci. Technol.* **2019**, *79*, 759–770. [[CrossRef](#)] [[PubMed](#)]
34. Corbellini, V.; Feng, C.; Bellucci, M.; Catenacci, A.; Stella, T.; Espinoza-Tofalos, A.; Malpei, F. Performance Analysis and Microbial Community Evolution of In Situ Biological Biogas Upgrading with Increasing H₂/CO₂ Ratio. *Archaea* **2021**, *2021*, 8894455. [[CrossRef](#)] [[PubMed](#)]
35. Díaz, I.; Fdz-Polanco, F.; Mutsvene, B.; Fdz-Polanco, M. Effect of operating pressure on direct biomethane production from carbon dioxide and exogenous hydrogen in the anaerobic digestion of sewage sludge. *Appl. Energy* **2020**, *280*, 115915. [[CrossRef](#)]
36. Khan, A.; Akbar, S.; Okonkwo, V.; Smith, C.; Khan, S.; Shah, A.A.; Adnan, F.; Ijaz, U.Z.; Ahmed, S.; Badshah, M. Enrichment of the hydrogenotrophic methanogens for, in-situ biogas up-gradation by recirculation of gases and supply of hydrogen in methanogenic reactor. *Bioresour. Technol.* **2022**, *345*, 126219. [[CrossRef](#)]
37. Kim, S.; Mostafa, A.; Im, S.; Lee, M.-K.; Kang, S.; Na, J.-G.; Kim, D.-H. Production of high-calorific biogas from food waste by integrating two approaches: Autogenerative high-pressure and hydrogen injection. *Water Res.* **2021**, *194*, 116920. [[CrossRef](#)]
38. Lebranchu, A.; Blanchard, F.; Fick, M.; Pacaud, S.; Olmos, E.; Delaunay, S. Pilot-scale biomethanation of cattle manure using dense membranes. *Bioresour. Technol.* **2019**, *284*, 430–436. [[CrossRef](#)]
39. Lovato, G.; Alvarado-Morales, M.; Kovalovszki, A.; Peprah, M.; Kougiyas, P.G.; Rodrigues, J.A.D.; Angelidaki, I. In-situ biogas upgrading process: Modeling and simulations aspects. *Bioresour. Technol.* **2017**, *245*, 332–341. [[CrossRef](#)]
40. Luo, G.; Angelidaki, I. Hollow fiber membrane based H₂ diffusion for efficient in situ biogas upgrading in an anaerobic reactor. *Appl. Microbiol. Biotechnol.* **2013**, *97*, 3739–3744. [[CrossRef](#)]
41. Luo, G.; Wang, W.; Angelidaki, I. Anaerobic digestion for simultaneous sewage sludge treatment and CO biomethanation: Process performance and microbial ecology. *Environ. Sci. Technol.* **2013**, *47*, 10685–10693. [[CrossRef](#)]
42. Treu, L.; Kougiyas, P.; de Diego-Díaz, B.; Campanaro, S.; Bassani, I.; Fernández-Rodríguez, J.; Angelidaki, I. Two-year microbial adaptation during hydrogen-mediated biogas upgrading process in a serial reactor configuration. *Bioresour. Technol.* **2018**, *264*, 140–147. [[CrossRef](#)]
43. Treu, L.; Tsapekos, P.; Peprah, M.; Campanaro, S.; Giacomini, A.; Corich, V.; Kougiyas, P.G.; Angelidaki, I. Microbial profiling during anaerobic digestion of cheese whey in reactors operated at different conditions. *Bioresour. Technol.* **2019**, *275*, 375–385. [[CrossRef](#)] [[PubMed](#)]
44. Voelklein, M.; Rusmanis, D.; Murphy, J. Biological methanation: Strategies for in-situ and ex-situ upgrading in anaerobic digestion. *Appl. Energy* **2019**, *235*, 1061–1071. [[CrossRef](#)]
45. Wahid, R.; Horn, S.J. Impact of operational conditions on methane yield and microbial community composition during biological methanation in in situ and hybrid reactor systems. *Biotechnol. Biofuels* **2021**, *14*, 1–15. [[CrossRef](#)] [[PubMed](#)]
46. Wahid, R.; Horn, S.J. The effect of mixing rate and gas recirculation on biological CO₂ methanation in two-stage CSTR systems. *Biomass Bioenergy* **2021**, *144*, 105918. [[CrossRef](#)]
47. Wahid, R.; Mulat, D.G.; Gaby, J.C.; Horn, S.J. Effects of H₂:CO₂ ratio and H₂ supply fluctuation on methane content and microbial community composition during in-situ biological biogas upgrading. *Biotechnol. Biofuels* **2019**, *12*, 1–15. [[CrossRef](#)]
48. Wang, W.; Xie, L.; Luo, G.; Zhou, Q.; Angelidaki, I. Performance and microbial community analysis of the anaerobic reactor with coke oven gas biomethanation and in situ biogas upgrading. *Bioresour. Technol.* **2013**, *146*, 234–239. [[CrossRef](#)]
49. Yang, Z.; Liu, Y.; Zhang, J.; Mao, K.; Kurbonova, M.; Liu, G.; Zhang, R.; Wang, W. Improvement of biofuel recovery from food waste by integration of anaerobic digestion, digestate pyrolysis and syngas biomethanation under mesophilic and thermophilic conditions. *J. Clean. Prod.* **2020**, *256*, 120594. [[CrossRef](#)]
50. Zhu, X.; Cao, Q.; Chen, Y.; Sun, X.; Liu, X.; Li, D. Effects of mixing and sodium formate on thermophilic in-situ biogas upgrading by H₂ addition. *J. Clean. Prod.* **2019**, *216*, 373–381. [[CrossRef](#)]
51. Zhu, X.; Chen, L.; Chen, Y.; Cao, Q.; Liu, X.; Li, D. Differences of methanogenesis between mesophilic and thermophilic in situ biogas-upgrading systems by hydrogen addition. *J. Ind. Microbiol. Biotechnol.* **2019**, *46*, 1569–1581. [[CrossRef](#)]
52. Zhu, X.; Chen, L.; Chen, Y.; Cao, Q.; Liu, X.; Li, D. Effect of H₂ addition on the microbial community structure of a mesophilic anaerobic digestion system. *Energy* **2020**, *198*, 117368. [[CrossRef](#)]
53. Bassani, I.; Kougiyas, P.G.; Angelidaki, I. In-situ biogas upgrading in thermophilic granular UASB reactor: Key factors affecting the hydrogen mass transfer rate. *Bioresour. Technol.* **2016**, *221*, 485–491. [[CrossRef](#)] [[PubMed](#)]
54. Jing, Y.; Campanaro, S.; Kougiyas, P.; Treu, L.; Angelidaki, I.; Zhang, S.; Luo, G. Anaerobic granular sludge for simultaneous biomethanation of synthetic wastewater and CO with focus on the identification of CO-converting microorganisms. *Water Res.* **2017**, *126*, 19–28. [[CrossRef](#)] [[PubMed](#)]
55. Deschamps, L.; Imatoukene, N.; Lemaire, J.; Mounkaila, M.; Filali, R.; Lopez, M.; Theoleyre, M.-A. In-situ biogas upgrading by bio-methanation with an innovative membrane bioreactor combining sludge filtration and H₂ injection. *Bioresour. Technol.* **2021**, *337*, 125444. [[CrossRef](#)]
56. Hafuka, A.; Fujino, S.; Kimura, K.; Oshita, K.; Konakahara, N.; Takahashi, S. In-situ biogas upgrading with H₂ addition in an anaerobic membrane bioreactor (AnMBR) digesting waste activated sludge. *Sci. Total Environ.* **2022**, *828*, 154573. [[CrossRef](#)] [[PubMed](#)]

57. Illi, L.; Lecker, B.; Lemmer, A.; Müller, J.; Oechsner, H. Biological methanation of injected hydrogen in a two-stage anaerobic digestion process. *Bioresour. Technol.* **2021**, *333*, 125126. [CrossRef]
58. Thapa, A.; Park, J.-G.; Yang, H.-M.; Jun, H.-B. In-situ biogas upgrading in an anaerobic trickling filter bed reactor treating a thermal post-treated digestate. *J. Environ. Chem. Eng.* **2021**, *9*, 106780. [CrossRef]
59. Corbellini, V.; Kougias, P.G.; Treu, L.; Bassani, I.; Malpei, F.; Angelidaki, I. Hybrid biogas upgrading in a two-stage thermophilic reactor. *Energy Convers. Manag.* **2018**, *168*, 1–10. [CrossRef]
60. Andreides, D.; Quispe, J.I.B.; Bartackova, J.; Pokorna, D.; Zabranska, J. A novel two-stage process for biological conversion of syngas to biomethane. *Bioresour. Technol.* **2021**, *327*, 124811. [CrossRef]
61. Scholten, J.C.; Conrad, R. Energetics of syntrophic propionate oxidation in defined batch and chemostat cocultures. *Appl. Environ. Microbiol.* **2000**, *66*, 2934–2942. [CrossRef]
62. Fontana, A.; Kougias, P.G.; Treu, L.; Kovalovszki, A.; Valle, G.; Cappa, F.; Morelli, L.; Angelidaki, I.; Campanaro, S. Microbial activity response to hydrogen injection in thermophilic anaerobic digesters revealed by genome-centric metatranscriptomics. *Microbiome* **2018**, *6*, 194. [CrossRef]
63. Batstone, D.J.; Keller, J.; Angelidaki, I.; Kalyuzhnyi, S.; Pavlostathis, S.; Rozzi, A.; Sanders, W.; Siegrist, H.; Vavilin, V. The IWA anaerobic digestion model no 1 (ADM1). *Water Sci. Technol.* **2002**, *45*, 65–73. [CrossRef] [PubMed]
64. Heaven, S.; Zhang, Y.; Bywater, A.; Banks, C. Dataset for 'Potential for Biomethanisation of CO₂ from Anaerobic Digestion of Organic Wastes in the UK'. 2022. Available online: https://eprints.soton.ac.uk/467644/1/processes_10_01202_1_.pdf (accessed on 6 June 2022).
65. Palù, M.; Peprah, M.; Tsapekos, P.; Kougias, P.; Campanaro, S.; Angelidaki, I.; Treu, L. In-situ biogas upgrading assisted by bioaugmentation with hydrogenotrophic methanogens during mesophilic and thermophilic co-digestion. *Bioresour. Technol.* **2022**, *348*, 126754. [CrossRef] [PubMed]

Disclaimer/Publisher's Note: The statements, opinions and data contained in all publications are solely those of the individual author(s) and contributor(s) and not of MDPI and/or the editor(s). MDPI and/or the editor(s) disclaim responsibility for any injury to people or property resulting from any ideas, methods, instructions or products referred to in the content.